

PROBING THE STANDARD MODEL AND
BEYOND WITH CP VIOLATION AND PARTICLE
COSMOLOGY

A Dissertation

Presented to the Faculty of the Graduate School

of Cornell University

in Partial Fulfillment of the Requirements for the Degree of

Doctor of Philosophy

by

Michael Paul Savastio

August 2015

PROBING THE STANDARD MODEL AND BEYOND WITH CP VIOLATION
AND PARTICLE COSMOLOGY

Michael Paul Savastio, Ph.D.

Cornell University 2015

We discuss topics related to CP violation and particle cosmology. First, we present some developments in improving the extraction of the CP violating parameter γ from the decay $B^\pm \rightarrow DK^\pm$ followed by the subsequent decay $D \rightarrow K_S \pi^+ \pi^-$. The mixing of the final state kaon is an additional CP violating effect which should be taken into account in the extraction of γ , and we discuss how this should be done. We also discuss the optimization of phase space binning needed to extract γ from these decays in a model independent way. Next, we discuss some cosmological constraints on R -parity violating, Minimally Flavor Violating (MFV) Supersymmetry (SUSY). Finally, we show that orbitally excited dark matter cannot persist over cosmic timescales for various model independent reasons.

BIOGRAPHICAL SKETCH

Michael Savastio was born in Port Jefferson, New York in 1987. After studying music at a performing arts school for a year following his graduation of high school, he began his study of physics at Stony Brook University in 2006. In 2008 he began working for Abhay Deshpande on various projects concerning the planning phase of eRHIC, a proposed upgrade to the Relativistic Heavy Ion Collider at Brookhaven National Laboratory. In May 2010 he received his bachelor degree from Stony Brook with a dual major in physics and mathematics. The following fall he began pursuing his PhD in physics at Cornell University. He returned to BNL in the summer of 2011 to continue working on the eRHIC project. In the summer of 2012 he began working for both Yuval Grossman in the Cornell Laboratory for Elementary Particle Physics theory group, as well as for Ritchie Patterson in the Cornell CMS experimental group. Choosing to specialize in high energy phenomenology, Savastio continued to work for Yuval Grossman (studying a wide variety of topics including CP violation, particle cosmology, and supersymmetry) until completing his PhD requirements in May 2015. In January of 2015 he began a fellowship at BNL, working for Grossman and Amarjit Soni on another project related to CP violation in heavy meson decays.

ACKNOWLEDGMENTS

I'd like to thank my adviser, Yuval Grossman, for useful discussions on physics topics, in addition to his excellent guidance and flexibility over the years. I'd also like to thank some others who have provided useful advice on physics topics appearing in this thesis: Maxim Perelstein, Amarjit Soni, Abner Soffer, Peter Lepage, Shmuel Nissovov, Mihailo Backovic and Ritchie Patterson. I'd also like to thank some of my fellow graduate students Jeff Dror, Nicolas Rey-Lorier, Michael Saelim and Philip Tanedo for useful discussions on physics topics. I'd like to thank some particularly influential course instructors I've had: Eanna Flanagan for his two semester general relativity course, Maxim Perelstein, Csaba Csaki, Yuval Grossman and Lawrence Gibbons for their instruction in quantum field theory and Standard Model related topics. Next I'd like to thank those who've helped me prior to my involvement at Cornell. Special thanks to Abhay Desphande, Elke Aschenauer and George Sterman. Thanks to all the others I've worked with during my time at BNL, and to many excellent instructors I had at Stony Brook. My work from January to May of 2015 was supported by the DOE Office of Science Graduate Student Research Fellowship.

TABLE OF CONTENTS

Biographical Sketch	iii
Acknowledgments	iv
Table of Contents	v
List of Tables	vii
List of Figures	viii
1 Improving the Extraction of γ from $B^\pm \rightarrow DK^\pm$	1
1.1 Pedagogical Introduction to CP Violation	1
1.1.1 CPV in the SM and the CKM Matrix	3
1.2 $K^0 - \bar{K}^0$ Mixing and Extracting γ from $B^\pm \rightarrow DK^\pm$	5
1.3 Gronau London Wyler (GLW) Method	6
1.4 The general case: Dalitz decays	8
1.4.1 General discussion	8
1.4.2 Including the kaon time dependence	12
1.4.3 Order $r_B \epsilon $ Terms	14
1.5 Assuming Breit-Wigner Dependence	15
1.6 Estimating the error in γ	18
1.7 Summary of $K^0 - \bar{K}^0$ Mixing in $B^\pm \rightarrow DK^\pm$	20
1.8 Improving $B^\pm \rightarrow DK^\pm$ Phase Space Binning	20
1.9 Giri Grossman Soffer Zupan (GGSZ) Fitting Method	21
1.10 Binning	23
1.10.1 Previous Optimal Binning Result	25
1.11 Proposed General Method for Optimizing Binning	26
1.11.1 Factorization Into Slowly Varying Functions	29
1.12 Results	31
1.12.1 Testing Previous Results	32
1.12.2 Un-Optimized Results	32
1.12.3 Optimized Results	33
1.13 Summary of Binning Improvement Results	34
2 Cosmological Constraints on MFV SUSY	37
2.1 Overview of MFV SUSY	37
2.2 Introduction to Cosmological Constraints on MFV SUSY	39
2.3 Pedagogical Review of Baryogenesis	40
2.3.1 Electroweak Baryogenesis	41
2.3.2 Leptogenesis	42
2.3.3 Affleck-Dine Baryogenesis	43
2.4 Baryogenesis Constraint on λ''	45
2.5 Gravitino DM in MFV SUSY	48
2.5.1 Anti-proton Constraints from PAMELA	49
2.5.2 γ -Ray Constraints from Fermi LAT	51
2.5.3 PAMELA e^+ Excess	53

2.6	Summary of Cosmological Constraints on MFV SUSY	53
3	The Fate of Orbitally Excited Dark Matter	56
3.1	Strongly-Interacting Dark Matter with Excited States	56
3.2	The model, notations and scales	57
3.3	Instability of highly excited states	60
3.4	Collisional De-excitation of Orbitally Excited States	63
3.4.1	Reheating through Collisional De-excitation	66
3.4.2	Relic Density of Excited States	67
3.5	Annihilation for excited states	68
3.6	Summary on Orbitally Excited Dark Matter	70
A	CPV Related Topics	71
A.1	Some Explicit Expressions for Kaon Mixing	71
A.2	Other Small Weak Phases	73
A.2.1	In $D \rightarrow K\pi^+\pi^-$	74
A.2.2	In $B^\pm \rightarrow DK^\pm$	74
A.3	Unbinned Analysis	75
A.4	Variational Calculus Approach for Improving Binning	76
A.5	BinOptimize Code	78
B	Orbitally Excited DM Appendix	79
B.1	Derivation of Boltzmann Equations	79
B.2	Thermal Average Cross-section	81
B.3	Model for Semi-Elastic De-excitation Interactions	82
B.4	Reheating Through Collisional De-exciation, Details	83
	Bibliography	85

LIST OF TABLES

1.1	Computed values for the binning quality factor Q when attempting to reproduce the results of [34], using the “ $\Delta\delta_D$ ” binning method.	32
1.2	Computed values of the quality factor R for binning in which the contours defining the binning have not been numerically optimized. The inequalities indicate that the bin shapes were symmetrized about $s_{12} = s_{13}$, for example ($s_{13} > s_{12}$) indicates that the bins in that region were mirrored about the line. ϕ indicates the physical value thereof.	32
1.3	The computed value of the quality factor R for various binnings. The same as Table 1.2 but after the contours defining the bin boundaries have been numerically optimized.	34
2.1	The representation of the MSSM quark and lepton superfields under the $SU(3)^5$ flavor group.	38
2.2	Multiplicities of protons or anti-protons for the final state relevant to MFV (cbs) and two others, from Pythia 8, for 100 GeV gravitinos. In parentheses are multiplicities reported by [63] to which we compare. We attribute the difference to the different versions of Pythia being used. We find that these values are nearly independent of the gravitino mass in the range of interest.	49
2.3	Comparison of multiplicities of final state photons from cbs and from $b\bar{b}$ as determined from Pythia 8 for 100 GeV gravitinos. Again, we find these values to be approximately independent of $m_{3/2}$ in the region of interest (for $m_{3/2} = 20$ GeV we have the cbs and $b\bar{b}$ multiplicities at about 8 and 13 respectively).	52
2.4	Comparison of multiplicities of final state electrons and positrons from cbs , $Z\nu$ and $W^\pm e^\mp$, found generating 10^4 events in Pythia 8 with $m_{3/2} = 100$ GeV.	52

LIST OF FIGURES

1.1	$\Delta\gamma$ (blue line) as a function of γ , as it appears in (1.62) for $\kappa'_D/F'_D = 1, r_B = 10^{-1}, \delta_B = \pi/2$. The shaded region represents an error due to $\delta(D_{0\infty}/N) = 0.01$. For kaon mixing to be relevant, uncertainty in the CP asymmetry $D_{0\infty}$ must be small enough that the blue line lies outside the shaded region.	19
1.2	The $B^+ \rightarrow (K_S \pi^+ \pi^-)_D K^+$ amplitude (arbitrary normalization). The large peaks are both from the K^+ resonance. The jagged edges are a result of interference between resonances.	35
1.3	The $\Delta\delta_D$ binning for $N = 40$. The ordinate represents the integral of the $B^+ \rightarrow DK^+$ amplitude over each bin.	36
1.4	Our binning method for $\phi = \pi/4$ and $N = 16$, without imposing symmetry. The ordinate represents integrals of the decay amplitude over each bin.	36
2.1	Upper limit on the gravitino mass as a function of $\tan(\beta)$ in order for it not to produce excessive \bar{p} or γ flux. Excluded regions are on the sides of the solid lines with hashing. The reason for the hard cutoff at $m_{3/2} = m_W$ in the $w'' = 0.01$ line is because the \bar{p} flux constraint is based on $\tilde{G} \rightarrow W^\pm \ell^\mp$	48
2.2	Comparison of anti-proton (left) and photon (right) spectra for various different final states generated using Pythia 8 and $m_{3/2} = 100$ GeV. The ordinate shows the number of particles, where 10^4 events were generated for each case. The shapes of the spectra were found to depend weakly on the gravitino mass in the region of interest (down to about m_W for anti-protons and about 20 GeV for photons).	50
2.3	Constraints on the MFV SUSY parameter space due to cosmological considerations. Excluded regions are on the sides of the lines with hashing. The region allowed by all constraints is highlighted in yellow. We show a possible bound from below assuming the \tilde{t} is the NLSP and requiring it not live more than 5 m so that it would not have been detected as a heavy stable charged particle at the LHC for two different values of $m_{\tilde{t}}$. (The limit of 5 m is taken so large in order to account for the possibility of low-velocity stops and is thought to be quite conservative.) . . .	55

CHAPTER 1

IMPROVING THE EXTRACTION OF γ FROM $B^\pm \rightarrow DK^\pm$

1.1 Pedagogical Introduction to CP Violation

We begin with a look into some specific phenomenological consequences of CP violation (CPV) in the Standard Model (SM). In order to predict these we must have some formal understanding of what the C and P operators are, in our case we are particularly interested on the effects on fermions. For an excellent and comprehensive review on CPV, see [1]. Standard quantum field theory texts can also be useful [2, 3].

Phenomenologically, CP violation means that

$$|\langle f|T|i\rangle| \neq |\langle \bar{f}|T|\bar{i}\rangle| \quad (1.1)$$

where T denotes the transition operator and \bar{i}, \bar{f} are the CP conjugate states of i, f (more about what that means will follow shortly). In order for CP violation to occur $\langle f|T|i\rangle$ and $\langle \bar{f}|T|\bar{i}\rangle$ must be expressible as the sum of multiple complex numbers, rather than just a single phase. This tells us that CP violation arises from interference between different Feynman diagrams.

A particularly nice formalism for understanding CP is that of the two-component Weyl spinors, see [4]. In four dimensions, ordinary Dirac spinors can be decomposed thus

$$\Psi(x) = \begin{pmatrix} \chi(x) \\ \eta^\dagger(x) \end{pmatrix} \quad (1.2)$$

where χ and η are independent two-component spinors. The separation of the four-component Dirac spinor into two two-component spinors reflects the

fact that the Lorentz algebra contains two commuting sub-algebras. Under the choice of basis where χ and η are in the fundamental representation of each of these sub-algebras, called the Weyl basis, the action of parity is

$$P : \quad \chi \leftrightarrow \eta^\dagger, \quad \eta \leftrightarrow \chi^\dagger \quad (1.3)$$

We can think of this as following from the fact that for massless fermions, χ and η have opposite helicity to χ^\dagger and η^\dagger while η has opposite charge from χ . The action of charge conjugation is then

$$C : \quad \chi \leftrightarrow \eta, \quad \chi^\dagger \leftrightarrow \eta^\dagger \quad (1.4)$$

To make these more vivid, consider the example of an electron ($\chi = e_L, \eta = e_R$). Then e_L is a left handed electron while e_R is a left handed positron. Likewise e_L^\dagger is a right handed positron while e_R^\dagger is a right handed electron. (The sub-indices L, R therefore correctly label the handedness of the *electron*, but are opposite for positrons.)

From the discussion above, we see that the action of CP is

$$CP : \quad \chi \leftrightarrow \chi^\dagger, \quad \eta \leftrightarrow \eta^\dagger \quad (1.5)$$

CP therefore exchanges Weyl spinors with their Hermitian conjugates, just as it does for scalars.

Let us now see how to build a Lagrangian which violates CP . Under the action of CP all of the scalars and fermions will be exchanged with their Hermitian conjugates. However, CP has no effect on the complex coefficients of operators. Therefore, suppose we have a Lagrangian containing a Yukawa term

$$\mathcal{L} \supset y\phi\chi\chi + y^*\phi^*\chi^\dagger\chi^\dagger \quad (1.6)$$

where ϕ is a scalar. Naively, it would seem that as long as the coupling y has a non-zero imaginary part, we will have CP violation. This is not quite true, however, since we could always redefine one or both of the fields such that y is purely real.

Consider now a case with three fields

$$\mathcal{L} \supset y_1 \phi \eta \chi + y_2 \phi \eta \eta + y_3 \phi \chi \chi + y_4 \phi^3 + \text{h.c.} \quad (1.7)$$

One may redefine the phase of the η field such that y_2 is purely real, the χ field such that y_3 is purely real and the ϕ field such that y_4 is purely real, but it is impossible to redefine the fields in such a way that all the y 's are purely real. The above Lagrangian therefore violates CP . Note that the phase of the complex y is precisely the phase which is different in the expression for $\langle \bar{f}|T|\bar{i} \rangle$ as opposed to $\langle f|T|i \rangle$ which allows for $|\langle \bar{f}|T|\bar{i} \rangle| \neq |\langle f|T|i \rangle|$. This is because the sign of this phase will now depend on whether a particular diagram involves particles or antiparticles.

We have seen that in order to achieve CP violation we needed more coupling constants than fields. As we will see, in the SM CP violation is only manifest when all three quark generations are involved. The reason is the same: with only two quark generations there are enough fields and few enough couplings that the couplings can all be made real, so that there is no CP violation.

1.1.1 CPV in the SM and the CKM Matrix

We have seen that a large number of couplings are required to produce a CP violating Lagrangian. The most likely culprit in the SM is then the quark and lepton

Yukawa couplings to the Higgs. These couplings are *a priori* unrestrained. The quark Yukawas can be written

$$\mathcal{L} \supset Y_{ij}^u \bar{Q}_i H d_j + Y_{ij}^d \bar{Q}_i H^\dagger u_j + \text{h.c.} \quad (1.8)$$

where $Q_i = (u_{Li}, d_{Li})$ is the left handed quark doublet and u_i and d_i are the right handed up and down quark fields respectively. The i, j 's denote flavor indices, while the color indices are suppressed for clarity. As stated previously the Yukawas Y_{ij}^u and Y_{ij}^d are not constrained by theory considerations. The presence of so many fields makes the determination of whether there is *CP* violation in the SM Yukawa sector in the most naive way rather complicated. Instead, to see where *CP* violation occurs lets rotate the quark fields into their mass bases, diagonalizing the Yukawas. We can always do this regardless of the form of Y_{ij}^u and Y_{ij}^d . In going to the mass basis the fields transform as $u_L \rightarrow V_L^u u_L$, $d \rightarrow V_R^d d$ et cetera. The cost of diagonalizing the Yukawas is that now the off-diagonal gauge couplings will now change

$$\mathcal{L} \supset \bar{u}_{Li} \mathcal{W}^+ (V_L^u V_L^{d\dagger})_{ij} d_{Lj} \quad (1.9)$$

Where $V = V_L^u V_L^{d\dagger}$ is the Cabbibo-Kobayashi-Maskawa (CKM) matrix. Note that it is manifestly unitary, since it is the product of two unitary basis transformation matrices.

An important self-consistency test of the SM is to ascertain whether the elements of the CKM matrix do indeed satisfy unitarity. One can do this by checking any of the N_f^2 equations

$$V_{ki} V_{kj}^* = \delta_{ij} \quad (1.10)$$

The weak decay widths and mixing parameters of various heavy mesons will depend on these constants. In particular, one may test the relation

$$V_{ud} V_{ub}^* + V_{cd} V_{cb}^* + V_{td} V_{tb}^* = 0 \quad (1.11)$$

This equation states that the sum of three complex numbers is a constant, and therefore has the geometrical interpretation of a triangle in the complex plane.

One can define the angles of this triangle

$$\alpha \equiv \arg\left(-\frac{V_{td}V_{tb}^*}{V_{ud}V_{ub}^*}\right) \quad (1.12)$$

$$\beta \equiv \arg\left(-\frac{V_{cd}V_{cb}^*}{V_{td}V_{tb}^*}\right) \quad (1.13)$$

$$\gamma \equiv \arg\left(-\frac{V_{ud}V_{ub}^*}{V_{cd}V_{cb}^*}\right). \quad (1.14)$$

For the CKM matrix to be unitary it is a necessary condition that $\alpha + \beta + \gamma = \pi$. Measuring all three of these angles therefore provides a test of the consistency of the SM.

1.2 $K^0 - \bar{K}^0$ Mixing and Extracting γ from $B^\pm \rightarrow DK^\pm$

Interference between the $b \rightarrow c\bar{u}s$ and $b \rightarrow u\bar{c}s$ decay amplitudes can be used to determine the weak phase γ . There are many hadronic final states that can be used to add information about γ [1, 5, 6, 7, 8, 9, 10] and, what is relevant to our case, some of them have one (or more) neutral kaon in the final state. All methods of determining γ from $B^\pm \rightarrow DK^\pm$ involve deriving a system of equations for γ in terms of the decay widths and amplitudes for the various processes involved. If all other quantities can be determined experimentally this allows for a model-independent determination of γ .

Thus far CP violation associated with neutral kaons in the determination of γ has been neglected since the effect is expected to be much smaller than current experimental uncertainties. As more statistics become available new sources of

CP violation in the overall process will become significant and will need to be taken into account. In this work we study the effects of CP violation in the kaon system on the determination of γ . Such effects were studied in other systems in [11, 12, 13, 14, 15, 16]. As we will see, there are effects that are linear in ϵ_K , and they are parametrically enhanced by $1/r_B$ (we use standard notations that are defined below). Once CP violation in the kaon system is included it is crucial that the time dependence of the kaon mixing be taken into account. This must be done in a way which considers time dependent detector efficiencies, and thus it can only be carried out by each experiment separately as part of their analysis.

1.3 Gronau London Wyler (GLW) Method

To understand the main issues associated with including kaon mixing and CPV effects, we start with the theoretically simplest case, which is the GLW method [5, 1]. We define

$$A(B^- \rightarrow D^0 K^-) = A(B^+ \rightarrow \bar{D}^0 K^+) \equiv A_B, \quad (1.15)$$

$$A(B^- \rightarrow \bar{D}^0 K^-) \equiv A_B r_B e^{i(\delta_B - \gamma)}, \quad A(B^+ \rightarrow D^0 K^+) \equiv A_B r_B e^{i(\delta_B + \gamma)}, \quad (1.16)$$

where δ_B is a strong phase and r_B is a real parameter which accounts for color and CKM suppression, and is measured to be of order 10^{-1} . We consider $D \rightarrow K\pi^0$ decays, but the π^0 can be exchanged for another CP eigenstate such as ρ^0 and the same discussion would apply. We further assume

$$|A(D^0 \rightarrow \bar{K}^0 \pi^0)| = |A(\bar{D}^0 \rightarrow K^0 \pi^0)|, \quad |A(D^0 \rightarrow K^0 \pi^0)| = |A(\bar{D}^0 \rightarrow \bar{K}^0 \pi^0)| = 0. \quad (1.17)$$

The decay $A(D^0 \rightarrow K^0 \pi^0)$ and its CP conjugate are doubly Cabbibo suppressed, and there is no real complication in including them, they are unimportant for

our current discussion, so for the moment we set them to zero (they are included in our final results). We also neglect terms of order $r_B|\epsilon_K|$ in this section for simplicity. For the kaons we use the standard notation

$$|K^0\rangle = \frac{1}{2p} (|K_L\rangle + |K_S\rangle), \quad |\bar{K}^0\rangle = \frac{1}{2q} (|K_L\rangle - |K_S\rangle), \quad \frac{A(K_L \rightarrow \pi\pi)}{A(K_S \rightarrow \pi\pi)} = \epsilon, \quad (1.18)$$

where in the last term we neglected direct CPV in kaon decays, that is, we set $\epsilon' = 0$. We define the time dependent asymmetry

$$a_{CP}(t) = \frac{\Gamma(B^+ \rightarrow (K_S\pi^0)_D K^+) - \Gamma(B^- \rightarrow (K_S\pi^0)_D K^-)}{\Gamma(B^+ \rightarrow (K_S\pi^0)_D K^+) + \Gamma(B^- \rightarrow (K_S\pi^0)_D K^-)}, \quad (1.19)$$

In the above t is the proper time of the kaon system, and by K_S we refer to a kaon that decays into two pions (see discussion in [16]). We work to first order in ϵ_K and we neglect terms of order $r_B|\epsilon_K|$ to find

$$a_{CP}(t) = \frac{2r_B \sin(\gamma) \sin(\delta_B) - 2\text{Re}(\epsilon) + 2e^{(\Gamma_S - \Gamma)t} \text{Re}(\epsilon^* e^{ix\Gamma t})}{1 + r_B^2 - 2r_B \cos(\gamma) \cos(\delta_B)}. \quad (1.20)$$

where as usual

$$\Gamma = \frac{\Gamma_S + \Gamma_L}{2}, \quad x = \frac{m_L - m_S}{\Gamma}. \quad (1.21)$$

It is useful to consider also the case where we integrate over the kaon lifetime. Following [16] we parametrize the experiment-dependent efficiency to detect the kaon by $F(t)$ with $0 \leq F(t) \leq 1$. We emphasize that F must be determined as part of the experimental analysis. We then define the time integrated asymmetry

$$A_{CP} = \frac{\int F(t) dt [\Gamma(B^+ \rightarrow (K_S\pi^0)_D K^+) - \Gamma(B^- \rightarrow (K_S\pi^0)_D K^-)]}{\int F(t) dt [\Gamma(B^+ \rightarrow (K_S\pi^0)_D K^+) + \Gamma(B^- \rightarrow (K_S\pi^0)_D K^-)]}, \quad (1.22)$$

where the integral is from zero to infinity. To demonstrate the effect we take a simple case where $F(t) = 1$ and we obtain

$$A_{CP} = \frac{2r_B \sin(\gamma) \sin(\delta_B) + 2\text{Re}(\epsilon)}{1 + r_B^2 - 2r_B \cos(\gamma) \cos(\delta_B)}. \quad (1.23)$$

We can check few limits of the above results:

1. For the case of no CPV in kaons, that is, $\epsilon \rightarrow 0$, and to first order in r_B we obtain

$$A_{CP} = 2r_B \sin(\gamma) \sin(\delta_B), \quad (1.24)$$

as we should.

2. The $r_B \rightarrow 0$ limit corresponds to the case where the only source of CP violation is in the kaon system. This case was studied for τ decays in [16]. Using Eq. (1.23) for $r_B \rightarrow 0$ we see that

$$A_{CP} = 2\text{Re}(\epsilon), \quad (1.25)$$

in agreement with [16].

3. Last we work to first order in r_B and we get

$$A_{CP} = 2r_B \left[\sin(\gamma) \sin(\delta_B) + \frac{\text{Re}(\epsilon)}{r_B} \right]. \quad (1.26)$$

Therefore, when both effects are included, A_{CP} (and therefore the extracted value of γ) is shifted by a term of order $\text{Re}(\epsilon)/r_B$. It is the $1/r_B$ enhancement which makes the effect larger and somewhere at the level that is expected to be probed in the near future.

1.4 The general case: Dalitz decays

1.4.1 General discussion

Our goal is to obtain a system of equations for γ in terms of various experimentally determined quantities in the most general case of a multi-body D decay such as $D \rightarrow K_S \pi^+ \pi^-$. The quantities involved will be integrated over finite

regions of the D decay phase space. Here we are using $D \rightarrow K_S \pi^+ \pi^-$ for concreteness, however our discussion will also apply to other decay modes such as $D \rightarrow K K^+ K^-$ and also to two-body decays, such as $D \rightarrow K_S \pi^0$, in which these amplitudes are not momentum dependent. We do not include other small effects like $D^0 - \bar{D}^0$ mixing which was discussed in [7, 17, 18, 19, 20]. Note that, though we will not discuss it further, it is imperative to include the effects of $D^0 - \bar{D}^0$ mixing since they will be competitive with those of CP violation in $K^0 - \bar{K}^0$ mixing.

With this in mind, we begin by defining quantities associated with the three-body D decay

$$\mathcal{A}(t) \equiv A(D^0 \rightarrow (\pi\pi)_K \pi^+ \pi^-) = A_{\pi\pi} \left(A_S e^{-im_S t - \Gamma_S t/2} + \epsilon A_L e^{-im_L t - \Gamma_L t/2} \right), \quad (1.27)$$

and its CP conjugate

$$\bar{\mathcal{A}}(t) \equiv A(\bar{D}^0 \rightarrow (\pi\pi)_K \pi^- \pi^+) = A_{\pi\pi} \left(\bar{A}_S e^{-im_S t - \Gamma_S t/2} + \epsilon \bar{A}_L e^{-im_L t - \Gamma_L t/2} \right), \quad (1.28)$$

where

$$A_{\pi\pi} \equiv A(K_S \rightarrow \pi\pi), \quad A_{S,L} \equiv A(D^0 \rightarrow K_{S,L} \pi^+ \pi^-), \quad \bar{A}_{S,L} \equiv A(\bar{D}^0 \rightarrow K_{S,L} \pi^- \pi^+), \quad (1.29)$$

and $\pi\pi$ is either of $\pi^+ \pi^-$ or $\pi^0 \pi^0$. Note that \mathcal{A} and $\bar{\mathcal{A}}$ are analogous to $A_D(s_{12}, s_{13})$ and $A_D(s_{13}, s_{12})$ of [7] respectively. We are assuming that we use the $\pi\pi$ final state to tag the kaon as a K_S and we have used (1.18). From now on meson variables such as p, q, ϵ, x, y will be for the K unless stated otherwise.

Interference of the \mathcal{A} and $\bar{\mathcal{A}}$ amplitudes will occur through the B^\pm decay, where the relative phase of the interference involves γ . With the definitions (1.15) and (1.16) we can write down the amplitude for the overall process in

terms of γ

$$A(B^- \rightarrow f^-) = A_B \left[\mathcal{A}(t) + r_B e^{i(\delta_B - \gamma)} \bar{\mathcal{A}}(t) \right], \quad f^\pm = [(\pi\pi)_{K\pi^+\pi^-}]_D K^\pm. \quad (1.30)$$

One can obtain the amplitude for the $B^+ \rightarrow f^+$ by $\gamma \rightarrow -\gamma$ and $\mathcal{A} \leftrightarrow \bar{\mathcal{A}}$. Squaring this we can write the time-dependent differential normalized widths

$$\begin{aligned} d\hat{\Gamma}(B^- \rightarrow f^-) &= |\mathcal{A}|^2 + r_B^2 |\bar{\mathcal{A}}|^2 + 2r_B \left[\text{Re}(\mathcal{A}^* \bar{\mathcal{A}}) \cos(\delta_B - \gamma) - \text{Im}(\mathcal{A}^* \bar{\mathcal{A}}) \sin(\delta_B - \gamma) \right], \\ d\hat{\Gamma}(B^+ \rightarrow f^+) &= |\bar{\mathcal{A}}|^2 + r_B^2 |\mathcal{A}|^2 + 2r_B \left[\text{Re}(\mathcal{A}^* \bar{\mathcal{A}}) \cos(\delta_B + \gamma) + \text{Im}(\mathcal{A}^* \bar{\mathcal{A}}) \sin(\delta_B + \gamma) \right], \end{aligned} \quad (1.31)$$

where $\hat{\Gamma} \equiv \Gamma/|A_B|^2$.

Eqs. (1.31) are our system of equations which can be used to determine γ . Note that $|\mathcal{A}|^2$ and $|\bar{\mathcal{A}}|^2$ are directly measurable in D decays. In addition to these there is a phase, that of $\mathcal{A}^* \bar{\mathcal{A}}$, which is momentum dependent in the multi-body case and which must be obtained in addition to r_B and δ_B in order to determine γ . These equations are identical in form to those from [7], and similar to those in [5] except that we distinguish between \mathcal{A} and $\bar{\mathcal{A}}$. The new complications are hidden in the time-dependence and CP violating parameters stored in \mathcal{A} and $\bar{\mathcal{A}}$.

We should proceed by setting up equations for the Dalitz analysis. This is performed by integrating over bins in the $D \rightarrow K_S \pi \pi$ phase space. First, let us define the momenta of the decay products and the Mandelstam variables as in [7]

$$K(p_1), \quad \pi^-(p_2), \quad \pi^+(p_3), \quad s_{ij} = (p_i + p_j)^2. \quad (1.32)$$

In the $\epsilon \rightarrow 0$ limit one has $\mathcal{A}(s_{12}, s_{13}) = \bar{\mathcal{A}}(s_{13}, s_{12})$. One way to think of this is that if the K_S were a CP eigenstate then $K_S \pi^+ \pi^-$ is a CP eigenstate but for momentum interchange. The effect due to the fact that the K_S is not a CP eigenstate is that $\mathcal{A}(s_{12}, s_{13}) = \bar{\mathcal{A}}(s_{13}, s_{12}) + O(|\epsilon|)$.

We would like to partition the (s_{12}, s_{13}) phase space into bins which are symmetric about the line $s_{12} = s_{13}$. With $\epsilon \rightarrow 0$ very simple relations exist between the various integrals above and below the $s_{12} = s_{13}$ line. The CP violation in the kaon system, however, complicates this. To this end, we define integrals over bins in phase space

$$T_i^-(t) \equiv \int_i d^2s |\mathcal{A}(t)|^2, \quad T_i^+(t) \equiv \int_i d^2s |\bar{\mathcal{A}}(t)|^2, \quad (1.33)$$

$$C_i(t) \equiv \int_i d^2s \operatorname{Re}(\mathcal{A}^* \bar{\mathcal{A}}), \quad S_i(t) \equiv \int_i d^2s \operatorname{Im}(\mathcal{A}^* \bar{\mathcal{A}}), \quad (1.34)$$

where we have emphasized that these quantities all depend on the proper time of the kaon. The index i labels a bin in (s_{12}, s_{13}) phase space, and we will let \bar{i} denote the bin obtained by reflecting the bin i about $s_{12} = s_{13}$. We can then write a system of equations for integrals of the overall decay width in these bins. At this stage we assume that we integrate over time, and we obtain

$$\hat{\Gamma}_i^- = T_i^- + r_B^2 T_i^+ + 2r_B [C_i \cos(\delta_B - \gamma) - S_i \sin(\delta_B - \gamma)], \quad (1.35)$$

$$\hat{\Gamma}_i^+ = T_i^+ + r_B^2 T_i^- + 2r_B [C_i \cos(\delta_B + \gamma) + S_i \sin(\delta_B + \gamma)]. \quad (1.36)$$

Note that the quantities T_i^\pm are the widths for $D \rightarrow K_S \pi^+ \pi^-$ with the K_S identified through its decay and thus can be determined from charm data, so we will treat these as known. In the $\epsilon \rightarrow 0$ limit we have $T_{\bar{i}}^- = T_i^+$. In contrast, the variables C_i and S_i arise from interference effects and therefore cannot be directly measured in non-interfering D decays.

Next we perform the counting of the number of observables and parameters to check if we can, in principle, obtain γ . We denote by k the number of bins above the $s_{12} = s_{13}$ line so that there are $2k$ bins in total. We consider n different B decay modes, such as $B \rightarrow D^{(*)} K^{(*)}$. We see that there are $2k$ C_i 's and $2k$ S_i 's, n of δ_B^f and r_B^f , and γ . We end up with $4k + 2n + 1$ unknowns and $4kn$ equations.

We see that for $n \geq 2$ we can find k such that there are more observables than unknowns and thus γ can be determined without any approximations.

We can also determine γ in the $n = 1$ case using approximations. One approximation is to use a model for the Dalitz plot. Another approximation that can be made is to take advantage of the fact that the main correction to γ comes from the term that is not proportional to r_B [see, Eq. (1.26)]. Thus, dropping terms of order $r_B|\epsilon|$ is equivalent to using $C_i = C_{\bar{i}}$ and $S_i = -S_{\bar{i}}$. In this case we have only $2k + 3$ unknowns with $4k$ equations which is solvable for $k \geq 2$.

Some other possibilities to reduce the number of unknowns were discussed in [7, 21, 22, 23, 24]. They are applicable here except that one must be careful to distinguish between CP conjugate quantities.

1.4.2 Including the kaon time dependence

When we outlined how methods for determining γ from $B^\pm \rightarrow DK^\pm$ can be adapted to include CP violation in the $K^0 - \bar{K}^0$ system we glossed over the time dependence of the kaon decay and oscillations by assuming we integrate over all of time. This is not realistic since time-dependent efficiencies must be taken into account. Below we discuss the time dependence issue in more detail.

We begin by writing the time dependence explicitly

$$|\mathcal{A}|^2 = |A_{\pi\pi}|^2 \left[|A_S|^2 e^{-\Gamma_S t} + 2e^{-\Gamma t} \text{Re} \left(\epsilon^* A_L^* A_S e^{ix\Gamma t} \right) \right], \quad (1.37)$$

$$|\bar{\mathcal{A}}|^2 = |A_{\pi\pi}|^2 \left[|\bar{A}_S|^2 e^{-\Gamma_S t} + 2e^{-\Gamma t} \text{Re} \left(\epsilon^* \bar{A}_L^* \bar{A}_S e^{ix\Gamma t} \right) \right], \quad (1.38)$$

$$\text{Re}(\mathcal{A}^* \bar{\mathcal{A}}) = \text{Re}(A_S^* \bar{A}_S) e^{-\Gamma_S t} + \text{Re} \left[\epsilon^* (A_S \bar{A}_L^* + A_L^* \bar{A}_S) e^{\Gamma t(ix-1)} \right], \quad (1.39)$$

$$\text{Im}(\mathcal{A}^* \bar{\mathcal{A}}) = \text{Im}(A_S^* \bar{A}_S) e^{-\Gamma_S t} + \text{Im} \left[\epsilon^* (A_L^* \bar{A}_S - A_S \bar{A}_L^*) e^{\Gamma t (ix-1)} \right], \quad (1.40)$$

where we have neglected the $|A_L|^2$ term as it is proportional to $|\epsilon|^2 \sim 10^{-6}$. In order to translate measurements performed in different timing windows, one must determine the various momentum dependent coefficients of the different time-dependent functions. For instance, we will need

$$\int dt F(t) |\mathcal{A}(t)|^2, \quad \int dt F(t) \text{Re}(\mathcal{A}^* \bar{\mathcal{A}}), \quad \int dt F(t) \text{Im}(\mathcal{A}^* \bar{\mathcal{A}}). \quad (1.41)$$

where $F(t)$ is the time-dependent detection efficiency defined above. To obtain such integrals we must determine both the real and imaginary parts of

$$|A_S|^2, \quad A_L^* A_S, \quad A_S^* \bar{A}_S, \quad A_S^* \bar{A}_L, \quad A_L^* \bar{A}_S \quad (1.42)$$

for each bin by distinguishing between the $\exp(-\Gamma_S t)$, $\exp(-\Gamma t) \cos(x\Gamma t)$, and $\exp(-\Gamma t) \sin(x\Gamma t)$ terms. When dropping order $r_B |\epsilon|$ terms only the first three of these need to be determined. (Some explicit expressions of time integrals can be found in Appendix A.)

While in principle knowing $F(t)$ will enable us to determine γ , care must be taken, as the whole program involves data from different experiments. For example, one uses charm decay data as an input to the B decay analysis. In principle $F(t)$ can be very different in such experiments, so naive use of this data introduces error. In practice, we expect $F(t)$ to be similar for different experiments so that the induced error will be small. Ultimately estimating this effect depends on the details of particular experiments, so this cannot be done in a general way.

1.4.3 Order $r_B|\epsilon|$ Terms

As we have already alluded to, there are complications that arise when terms of order $r_B|\epsilon|$ are included. This is because there is a new variable (roughly speaking it is the phase of $A_S^*\bar{A}_S$) which only appears in interference between D^0 and \bar{D}^0 amplitudes. To understand how these terms complicate the analysis, we should introduce new definitions. First, we define

$$A_D \equiv A(D^0 \rightarrow \bar{K}^0 \pi^+ \pi^-), \quad A_D r_D e^{i\delta_D} \equiv A(D^0 \rightarrow K^0 \pi^+ \pi^-), \quad (1.43)$$

and the CP conjugate amplitudes

$$\bar{A}_D \equiv A(\bar{D}^0 \rightarrow K^0 \pi^- \pi^+), \quad \bar{A}_D \bar{r}_D e^{i\bar{\delta}_D} \equiv A(\bar{D}^0 \rightarrow \bar{K}^0 \pi^- \pi^+). \quad (1.44)$$

We emphasize that A_D , r_D , δ_D and their conjugates depend on (s_{12}, s_{13}) for multi-body decays. Here r_D is a CKM suppression factor, but we do not know how small it is in any particular region of phase space. From here on we neglect CP violation in the D decay, and then we have

$$A_D(s_{12}, s_{13}) = \bar{A}_D(s_{13}, s_{12}), \quad r_D(s_{12}, s_{13}) = \bar{r}_D(s_{13}, s_{12}), \quad \delta_D(s_{12}, s_{13}) = \bar{\delta}_D(s_{13}, s_{12}). \quad (1.45)$$

(In principle A_D , r_D , δ_D are each measurable through flavor specific decays of the kaon, for example, $D^0 \rightarrow (\pi \ell^+ \nu)_K \pi^+ \pi^-$ and its CP conjugates.) From these we find

$$A_S = \frac{A_D}{2pq} (qr_D e^{i\delta_D} - p) = \frac{A_D}{\sqrt{2}} \left((1 - \epsilon) r_D e^{i\delta_D} - 1 - \epsilon \right) + O(|\epsilon|^2), \quad (1.46)$$

$$A_L = \frac{A_D}{2pq} (qr_D e^{i\delta_D} + p) = \frac{A_D}{\sqrt{2}} \left((1 - \epsilon) r_D e^{i\delta_D} + 1 + \epsilon \right) + O(|\epsilon|^2), \quad (1.47)$$

The CP conjugate expressions for $\bar{A}_{S,L}$ are obtained by $A_D \rightarrow \bar{A}_D$, $\epsilon \rightarrow -\epsilon$, and $A_S \rightarrow -A_S$. The phase between p and q is unphysical but we adopt the convention $q = (1 - \epsilon)/\sqrt{2}$ and $p = (1 + \epsilon)/\sqrt{2}$. The new phase which occurs only in the

r_B terms which cannot be obtained through measurements of non-interfering D decays alone is that of $A_D^* \bar{A}_D$ so we define

$$\theta_D(s_{12}, s_{13}) \equiv \arg(A_D^* \bar{A}_D). \quad (1.48)$$

Under an interchange of the pion momenta one has $\theta_D \rightarrow -\theta_D$. The value of this angle at a point in phase space is unphysical, but for a particular choice of δ_B it is fixed, and its momentum dependence is physical. It reduces to $\delta_{12,13} - \delta_{13,12}$ of [7] in the $\epsilon \rightarrow 0$ limit.

If one expands out the real and imaginary parts of $\mathcal{A}^* \bar{\mathcal{A}}$ one will obtain various combinations of $|A_D|^2, r_D, \delta_D$ and trig functions of $\theta_D, \delta_D, \bar{\delta}_D$ such as $r_D \cos(\theta - \delta_D), \bar{r}_D \cos(\theta + \bar{\delta}_D),$ and $r_D \bar{r}_D \cos(\theta + \bar{\delta}_D - \delta_D)$. These are of course multiplied by $|A_D \bar{A}_D|$ and are ultimately integrated over bins of phase space. The full result can be found in Appendix A.

1.5 Assuming Breit-Wigner Dependence

As we alluded to previously, some unknowns can be eliminated by assuming a Breit-Wigner dependence for the D decays. The change one needs to keep in mind when generalizing the discussion of Breit-Wigner dependence from a case where kaon CP violation is neglected is that CP conjugate amplitudes are no longer related by only an exchange of pion momenta.

We substitute A_S above with a sum over Breit-Wigner functions

$$A_S(s_{12}, s_{13}) = a_0 e^{i\delta_0} + \sum_r a_r e^{i\delta_r} A_r(s_{12}, s_{13}), \quad (1.49)$$

where

$$A_r(s_{12}, s_{13}) = {}^J \mathcal{M}_r W^r, \quad (1.50)$$

and the index r labels the resonance. The factor ${}^J\mathcal{M}_r$ depends on the spin of the resonance, for example ${}^0\mathcal{M}_r = 1$, ${}^1\mathcal{M}_r = -2\vec{k}_1 \cdot \vec{k}_2$ where \vec{k}_1, \vec{k}_2 are the spatial momenta of the particles originating from the resonance. The Breit-Wigner function is

$$W^r = \frac{1}{s - M_r^2 + iM_r\Gamma_r(\sqrt{s})}, \quad (1.51)$$

where M_r is the mass of the resonance. The argument of W^r depends on the particles which participate in the resonance, for example for the ρ^0 the argument of W^r is s_{23} . Explicit expressions for the mass dependent width $\Gamma_r(\sqrt{s})$ and the other ${}^J\mathcal{M}_r$'s can be found in [25, 26, 27, 28].

In order to account for CP violation in the kaon system one cannot assume that the amplitudes are related to their CP conjugates by a momentum exchange alone, for instance

$$a_\rho \propto A(D^0 \rightarrow \rho^0 K_S) \neq \bar{a}_\rho \propto A(\bar{D}^0 \rightarrow \rho^0 K_S). \quad (1.52)$$

The reason for this is that the K_S is not an exactly even superposition of K^0 and \bar{K}^0 . Fortunately, these are related through simple momentum independent factors

$$A(D^0 \rightarrow \rho^0 K_S) = \frac{A_\rho}{2pq}(qR_\rho - p) = \frac{A_\rho}{\sqrt{2}}(R_\rho - \epsilon R_\rho - 1 - \epsilon) + O(|\epsilon|^2), \quad (1.53)$$

$$A(\bar{D}^0 \rightarrow \rho^0 K_S) = \frac{A_\rho}{2pq}(q - pR_\rho) = \frac{A_\rho}{\sqrt{2}}(1 - \epsilon - R_\rho - \epsilon R_\rho) + O(|\epsilon|^2), \quad (1.54)$$

where $A_\rho \equiv A(D^0 \rightarrow \rho^0 \bar{K}^0)$, $A_\rho R_\rho \equiv A(D^0 \rightarrow \rho^0 K^0)$ with R_ρ complex and we have neglected CP violation in the D decay so that $A(D^0 \rightarrow \rho^0 \bar{K}^0) = A(\bar{D}^0 \rightarrow \rho^0 K^0)$. Similar expressions apply for any resonance decay of the form $D^0 \rightarrow K_S X$.

The situation is slightly different for decays in which the K_S emerges from a resonance such as $D^0 \rightarrow K^{*-}\pi^+$. In this case

$$a_{K^*} \propto A(D^0 \rightarrow K^{*-}\pi^+) \neq \bar{a}_{K^*} \propto A(\bar{D}^0 \rightarrow K^{*+}\pi^-) \quad (1.55)$$

because $A(K^{*-} \rightarrow K_S \pi^-) \neq A(K^{*+} \rightarrow K_S \pi^+)$. Fortunately, these are again simply related by momentum-independent factors

$$A(K^{*-} \rightarrow K_S \pi^-) = -\frac{A_*}{2q} = -\frac{A_*}{\sqrt{2}}(1 + \epsilon), \quad (1.56)$$

$$A(K^{*+} \rightarrow K_S \pi^+) = \frac{A_*}{2p} = \frac{A_*}{\sqrt{2}}(1 - \epsilon), \quad (1.57)$$

where $A_* = A(K^{*-} \rightarrow \bar{K}^0 \pi^-) = A(K^{*+} \rightarrow K^0 \pi^+)$ and we have assumed $\Delta(\text{strangeness}) = 2$ decays to be forbidden entirely. In this way one can relate a_{K^*} to \bar{a}_{K^*} .

For $\epsilon \rightarrow 0$ one only has the amplitude A_S , but for finite ϵ , we also have A_L , which can be decomposed just like (1.49). The same discussion on how to account for CP violation applies, however the relation between some of the coefficients is different. A general procedure for relating amplitude coefficients is as follows

1. Express decay amplitudes in terms of $A(D \rightarrow KX)$ for resonances which do not decay to the final state neutral kaon, where K is one of K^0, \bar{K}^0 .
2. Express decay amplitudes in terms of $A(X_S \rightarrow KX)$ where X_S is a resonance which decays to a neutral kaon.
3. Project out the $K_{S,L}$ component using the reciprocal basis

$$\langle K_{L,S} | = \frac{1}{p} \langle K^0 | \pm \frac{1}{q} \langle \bar{K}^0 | \quad (1.58)$$

to relate the various coefficients.

where the + is for the K_L and the - is for the K_S .

1.6 Estimating the error in γ

Next we estimate the error introduced on the extracted value of γ if one were to use the standard analysis and neglect CP violation in the kaon system. We do so by making the following simplifying assumptions: We neglect terms of order $r_B|\epsilon|$, we assume that we integrate over all of the $K_S\pi^+\pi^-$ phase space, and we assume that $F(t) = 1$. A simple expression for γ can be obtained in terms of the difference

$$D_{0\infty} = \int_0^\infty dt \left[\Gamma(B^+ \rightarrow (\pi^4)_D K^+) - \Gamma(B^- \rightarrow (\pi^4)_D K^-) \right]. \quad (1.59)$$

Inverting the result for $D_{0\infty}$ one finds

$$\sin(\gamma) = \frac{D_{0\infty}/N - 4\kappa'_D \text{Re}(\epsilon)}{4r_B F'_D \sin(\delta_B)}. \quad (1.60)$$

where $N \equiv |A(K_S \rightarrow \pi\pi)A_B|^2/2\Gamma_S$ and F'_D and κ'_D are functions of A_D, r_D, δ_D and $\bar{A}_D, \bar{r}_D, \bar{\delta}_D$ which are defined in Appendix A. Next we define

$$\Delta\gamma \equiv \gamma - \gamma_0, \quad (1.61)$$

where γ_0 is γ as determined from A_{CP} with $\epsilon = 0$. We find

$$\Delta\gamma = -\frac{\kappa'_D \text{Re}(\epsilon)}{r_B F'_D \cos(\gamma_0) \sin(\delta_B)}, \quad (1.62)$$

and we expect $\kappa'_D/F'_D \sim 1$. To see this, note that in the limit where we neglect doubly Cabbibo suppressed D decays and let the D decay to a true CP eigenstate one obtains the same expression for $\Delta\gamma$ with $\kappa'_D/F'_D = 1$. Therefore we find $\Delta\gamma \sim |\epsilon|/r_B$.

There appear to be several limits in which $\Delta\gamma$ diverges. The first type is when any of r_B, F'_D , or δ_B vanish. None of these are problematic since they arise

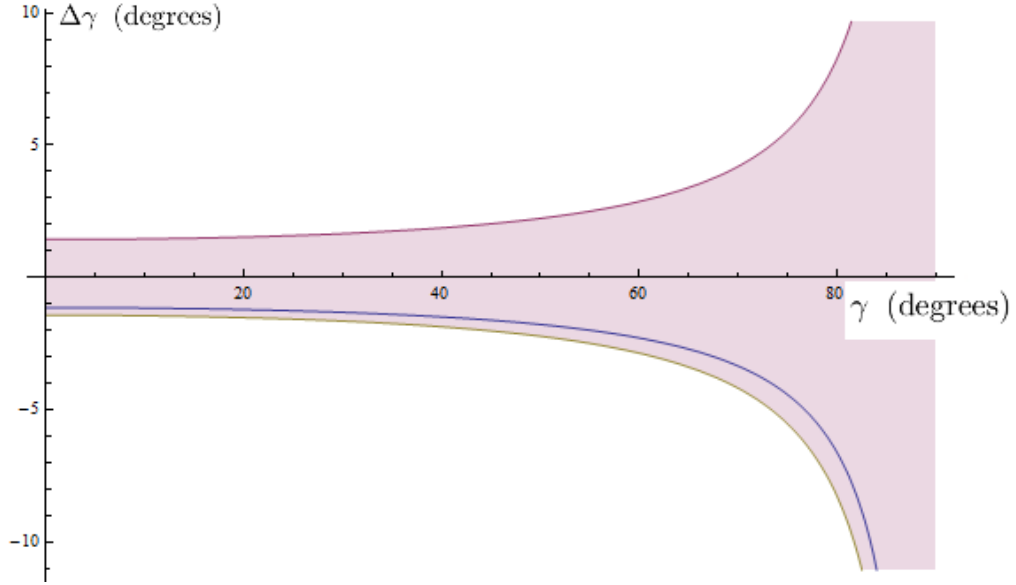


Figure 1.1: $\Delta\gamma$ (blue line) as a function of γ , as it appears in (1.62) for $\kappa'_D/F'_D = 1$, $r_B = 10^{-1}$, $\delta_B = \pi/2$. The shaded region represents an error due to $\delta(D_{0\infty}/N) = 0.01$. For kaon mixing to be relevant, uncertainty in the CP asymmetry $D_{0\infty}$ must be small enough that the blue line lies outside the shaded region.

only when working to leading order, which is no longer justified in that case.

Keeping the full expression we find

$$\frac{\sin(\gamma_0 + \Delta\gamma) - \sin(\gamma_0)}{\sin(\gamma_0)} = -\frac{4\kappa'_D \text{Re}(\epsilon)}{D_{0\infty}/N}, \quad (1.63)$$

which does not depend on r_B , F'_D , or δ_B . Next we see that $\Delta\gamma$ appears to diverge for $\gamma_0 \rightarrow \pi/2$. This divergence reflects the fact that $D_{0\infty}$ depends only very weakly on γ for $\gamma \approx \pi/2$. Therefore, any source of error in $D_{0\infty}/N$ would also cause a large shift in γ in this region. The uncertainty in γ using this method is then large for $\gamma \approx \pi/2$, so we expect that $\Delta\gamma$ is also large there. This uncertainty is only intrinsic to the Dalitz method where S_i is small. Where C_i is small there is a similar uncertainty near $\gamma \approx 0$. The effect is demonstrated in Fig. 1.1.

The best current determinations of γ from Belle and BaBar have uncertainties of roughly $\pm 10^\circ$ [27, 26]. We expect $|\Delta\gamma|$ to be of order $\text{Re}(\epsilon)/r_B \approx 1^\circ$ so it may

be some time before the effect of CP violation in kaon mixing and decay becomes relevant. This correction is, however, very large compared to the largest irreducible theoretical error on the determination of γ from $B \rightarrow DK$ [29].

1.7 Summary of $K^0 - \bar{K}^0$ Mixing in $B^\pm \rightarrow DK^\pm$

The $B \rightarrow DK$ program is known to have the smallest theoretical error in any determination of weak parameters [29]. As precision improves it becomes more important to look for sub-leading effects [30, 31]. We generalized the $B \rightarrow DK$ method for determining γ to account for additional sources of CP violation from mixing of final state neutral kaons. We found that γ is shifted by an amount of order $\epsilon/r_B \sim 10^{-2}$. While this effect is still below the current experimental sensitivity, it may be important in the near future. We have discussed how existing methods can be corrected to account for this effect.

1.8 Improving $B^\pm \rightarrow DK^\pm$ Phase Space Binning

As a new generation of high luminosity quarkonia factories such as LHCb and Belle2 [33] begin to perform analyses on data, it is vital to ensure that the available techniques for extracting the weak angles do not impose theoretical or systematic limitations on the precision of their measurements. Extremely precise measurements of β have been achieved utilizing the decay $B^0 \rightarrow J/\psi K_S$. So far the least well constrained of the CKM weak angles is γ , and it is desirable to increase the precision of its measurement to be on par with that of β so as to test the self-consistency of the SM and indirectly search for new physics. The inter-

ference between $b \rightarrow c\bar{u}s$ and $b \rightarrow \bar{c}us$ amplitudes which appear in the decays $B^\pm \rightarrow DK^\pm$ can be used to determine γ in a clean way not contaminated by the contributions of penguin diagrams. Various methods for extracting γ from these decays have been developed. The method which has achieved the most precise measurements of γ to date and involves a Dalitz plot analysis of three-body D decays such as $D \rightarrow K\pi^+\pi^-$ or $D \rightarrow KK^+K^-$ [7]. Determination of γ via this method requires the measurement of the phase space distribution of the three-body D decays to eliminate strong phases in a model-independent way. In practice, this involves segregating the phase space into bins and counting events. Since the phase space distribution of the decays is highly non-uniform, the precision with which γ can be determined using this method depends strongly on the shape of the phase space bins. Extremely fine binning is undesirable because some bins would be extremely underpopulated even with very high statistics. In what follows we attempt to find the binning which maximizes the statistical sensitivity to γ for a fixed number of bins.

1.9 Giri Grossman Soffer Zupan (GGSZ) Fitting Method

A model independent way of obtaining γ from measurements of the D decay subsequent to $B^\pm \rightarrow DK^\pm$ has been introduced in [7]. The most accurate measurements of γ to this date have been obtained by using this method [30].

In the decay, the B meson decays into a superposition of $D^0 - \bar{D}^0$ states which depends on the weak angle γ . This D state then decays, for our purposes we consider only the decays into three-body states such as $K_S\pi^+\pi^-$. The overall

amplitude for $B^+ \rightarrow (K_S \pi^+ \pi^-)_D K^+$ can then be written

$$A_B(s_{12}, s_{13}) = A_D(s_{12}, s_{13}) + r_B e^{i\phi_+} \bar{A}_D(s_{12}, s_{13}) \quad (1.64)$$

where s_{12} is the invariant mass of $K_S \pi^+$, s_{13} is the invariant mass of $K_S \pi^-$ and $\phi_{\pm} \equiv \delta_B \pm \gamma$ where δ_B is the strong (non CP violating) part of the phase between the D decay amplitudes. Here A_D is the amplitude for $\bar{D}^0 \rightarrow K_S \pi^+ \pi^-$ while \bar{A}_D is the amplitude for $D^0 \rightarrow K_S \pi^+ \pi^-$. The parameter r_B is a CKM and color suppression factor, found to be $r_B \sim 10^{-1}$ [7]. Because the K_S is a CP eigenstate, neglecting CP violation in D mixing and decay we have

$$A_D(s_{12}, s_{13}) = \bar{A}_D(s_{13}, s_{12}) \quad (1.65)$$

As we will see, this relationship allows us to greatly reduce the number of parameters which need to be fitted.

Following the notation of [34], the squared amplitude can be written

$$f_+ = p + r_B^2 \bar{p} + 2 \sqrt{p \bar{p}} (x_+ c + y_+ s) \quad (1.66)$$

where

$$p(s_{12}, s_{13}) = |A_D(s_{12}, s_{13})|^2 \quad \bar{p}(s_{12}, s_{13}) = |\bar{A}_D(s_{12}, s_{13})|^2 \quad (1.67)$$

$$x_{\pm} = r_B \cos(\phi_{\pm}) \quad y_{\pm} = r_B \sin(\phi_{\pm}) \quad (1.68)$$

and c, s are the cosine and sine, respectively, of $\Delta\delta_D$, the phase of $A_D \bar{A}_D^*$. Using (1.65) we can easily obtain the squared amplitude for the B^- decay

$$f_- = \bar{p} + r_B^2 p + 2 \sqrt{p \bar{p}} (x_- c - y_- s) \quad (1.69)$$

Note that the f' s are simply probability density functions to obtain an event at phase space location $\vec{s}_i = (s_{12}^i, s_{13}^i)$.

To determine γ , one needs to integrate over bins, and fit for ϕ_{\pm} . Performing such an integral one obtains

$$F_i^+ = P_i + r_B^2 \bar{P}_i + 2 \sqrt{P_i \bar{P}_i} (x_+ c_i + y_+ s_i) \quad (1.70)$$

$$F_i^- = \bar{P}_i + r_B^2 P_i + 2 \sqrt{P_i \bar{P}_i} (x_- c_i - y_- s_i) \quad (1.71)$$

where $P_i = \int_i d^2 s p$, $\bar{P}_i = \int_i d^2 s \bar{p}$ are integrals over the i th bin and

$$c_i = \frac{1}{\sqrt{P_i \bar{P}_i}} \int_i d^2 s \sqrt{p_D \bar{p}_D} \cos(\Delta\delta_D) \quad (1.72)$$

$$s_i = \frac{1}{\sqrt{P_i \bar{P}_i}} \int_i d^2 s \sqrt{p_D \bar{p}_D} \sin(\Delta\delta_D) \quad (1.73)$$

Now suppose we have an even number of bins such that the binning is symmetric about the line $s_{12} = s_{13}$. The relation (1.65) allows us to relate F_i^+ and F_i^- . Let the bins be labeled such that the bins $i > 0$ lie in the region $s_{12} > s_{13}$ and the bins $i < 0$ lie in the region $s_{13} > s_{12}$. Then

$$F_{-i}^+ = P_i + r_B^2 P_{-i} + 2 \sqrt{P_i P_{-i}} (x_+ c_i + y_+ s_i) \quad (1.74)$$

$$F_{-i}^- = P_{-i} + r_B^2 P_i + 2 \sqrt{P_i P_{-i}} (x_- c_i - y_- s_i) \quad (1.75)$$

Note that by definition $c_i = c_{-i}$ and $s_i = -s_{-i}$. Thanks to these symmetries, for N bins we only need to fit for the $2N + 3$ variables P_i , c_i , s_i , r_B and ϕ_{\pm} .

1.10 Binning

In the previous section we have indicated how one might use a binned likelihood fit to obtain γ from $B^{\pm} \rightarrow (K_S \pi^+ \pi^-) K^{\pm}$. In practice, even modern B factories only obtain a few thousand usable events [37]. Of course, in principle one would like to use as many bins as possible to reduce the statistical error, provided one

has enough data, but the fact that the D decay phase space is so strongly dominated by a few resonances (in particular K_*^\pm) would leave a naive fine binned approach with a large number of unpopulated or underpopulated bins. This would have the effect of introducing more unknowns to the fit without introducing new data, and is therefore undesirable. To resolve this, it is necessary to use a relatively coarse binning with bin shapes which maximize the statistical sensitivity to γ . This approach was first explored in [34] and experimental collaborations have been employing it since.

Our goal has bin to improve upon the result of [34]. We will discuss why this seems likely to be possible in the next section. For now, we want to see how to obtain the statistical sensitivity of a given binning. To this end, we assume there is only one variable which needs to be fitted for for each of $B^+ \rightarrow DK^+$ and $B^- \rightarrow DK^-$, in particular ϕ_+ and ϕ_- respectively. Of course $\gamma = (\phi^+ - \phi^-)/2$ and its statistical uncertainty is related in a simple way to the uncertainties in ϕ_+ and ϕ_- so it is clear that a method which maximizes the sensitivity to ϕ_+, ϕ_- will maximize the sensitivity to γ . Considering this, unless otherwise specified we will discuss the uncertainty in ϕ (either ϕ_+ or ϕ_-). It is far from true that the only variable which needs to be fitted for is ϕ , our only handle for adjusting the covariance matrix is the binning, and the variables we are fitting are, in general, badly model dependent, so it would gain us little to consider the general case, while making any analysis enormously more complex.

Then, the standard likelihood fitting analysis gives us

$$\langle \sigma_\phi^2 \rangle^{-1} = -\frac{\partial^2 \log(L(\phi))}{\partial \phi^2} = \sum_{i=1}^N \frac{1}{F_i} \left(\frac{\partial F_i}{\partial \phi} \right)^2 \quad (1.76)$$

where $L(\phi)$ is the likelihood function. We have used the fact that the probability to obtain a given number of events in a given bin is Poisson distributed. The

average brackets denote that this is an average over all experiments, i.e. that if one has performed a large number of independent experiments to determine ϕ , its average inverse variance is given by the above (henceforth we'll drop these brackets for convenience). This is therefore the quantity that we wish to choose binning which maximizes. It is useful to compare this to an ideal case. If we suppose that we have infinitely many bins, the sensitivity approaches

$$\sigma_\phi^{-2} \rightarrow \int d^2s \frac{1}{f} \left(\frac{\partial f}{\partial \phi} \right)^2 \quad (1.77)$$

This is the maximum theoretical sensitivity obtainable from a binned approach, and is related in a complicated way to the unbinned sensitivity (see Appendix A). We then define the quality factor

$$R^2 = \sum_{i=1}^N \frac{1}{F_i} \left(\frac{\partial F_i}{\partial \phi} \right)^2 \left(\int d^2s \frac{1}{f} \left(\frac{\partial f}{\partial \phi} \right)^2 \right)^{-1} \quad (1.78)$$

We therefore wish to find the binning which maximizes R , where $R < 1$.

1.10.1 Previous Optimal Binning Result

The problem of optimizing the bin shape to maximize sensitivity to γ was first approached in [34]. Several factors led us to believe it likely that this result could be improved upon. First, the binning was optimized by considering the sensitivity to x and y , using the quality factor

$$Q^2 = \sum_{i=1}^N \left(\frac{1}{F_i} \left(\frac{\partial F_i}{\partial x} \right)^2 + \frac{1}{F_i} \left(\frac{\partial F_i}{\partial y} \right)^2 \right) \left[\int d^2s \left(\frac{1}{f} \left(\frac{\partial f}{\partial x} \right)^2 + \frac{1}{f} \left(\frac{\partial f}{\partial y} \right)^2 \right) \right]^{-1} \quad (1.79)$$

which is analogous to (1.78) for x and y . It does not seem to be in general true that maximizing Q^2 maximizes R^2 , but certainly the two are closely related. In [34] it was shown that for $x = y = 0$ if the relation $c_i^2 + s_i^2 = 1$ is satisfied, one

obtains perfect binning (equivalent to having infinite bins). This is the result of a special cancellation, which does not occur in the more general case. Additionally, the condition $x = y = 0$ is, of course, inconsistent with the definitions of x, y which was justified in [34] by the fact that f depends weakly on x and y . As we will see, there are deeper, more general reasons why binning which nearly satisfies $s_i^2 + c_i^2 = 1$ is nearly optimal. For now, we point out that binning which nearly satisfies this relation greatly simplifies the extraction of the s_i parameters from other D decay experiments, a benefit which will outweigh the advantage of binning with slightly better R but which badly violates $s_i^2 + c_i^2 = 1$.

1.11 Proposed General Method for Optimizing Binning

As we have seen the quality factor R depends on various integrals of the probability distribution function f over the phase space. One may think of R as being written in terms of averages of f and various functions of it.

Let's define an average in the usual way

$$\langle f \rangle_i = \frac{1}{A_i} \int_i d^2\xi f \quad (1.80)$$

where A_i is the area of the i th bin. We have relabeled the phase space parameters ξ_{12}, ξ_{13} to avoid confusion with $s = \sin(\Delta\delta_D)$. Of course $\partial/\partial\phi$ commutes with $\langle \cdot \rangle$. With this we can express (exactly)

$$R^2 = \left(\sum_{i=1}^N \frac{1}{\langle f \rangle_i} \left\langle \frac{\partial f}{\partial \phi} \right\rangle_i^2 \right) \left(\sum_{i=1}^N \left\langle \frac{1}{f} \left(\frac{\partial f}{\partial \phi} \right)^2 \right\rangle_i \right)^{-1} \quad (1.81)$$

It seems intuitively obvious that ideally we'd like both f and its derivative vary as little as possible in each bin since for the case where they are exactly constant

in each bin $R^2 = 1$ (i.e. is maximized). We express the denominator in terms of $\langle f \rangle$ and $\langle \partial f / \partial \phi \rangle$.

To this end, let's define for each bin

$$f(\vec{s}) = \langle f \rangle + \delta f(\vec{\xi}) \quad (1.82)$$

where $\delta f = f(\vec{\xi}) - \langle f \rangle$ is small everywhere in the bin as long as the standard deviation of f everywhere in the bin is sufficiently small. We can then expand

$$\frac{1}{f} \left(\frac{\partial f}{\partial \phi} \right)^2 = \left(\frac{1}{\langle f \rangle} - \frac{1}{\langle f \rangle^2} \delta f + \frac{1}{\langle f \rangle^3} \delta f^2 \right) \left(\left\langle \frac{\partial f}{\partial \phi} \right\rangle^2 + 2 \left\langle \frac{\partial f}{\partial \phi} \right\rangle \frac{\partial \delta f}{\partial \phi} + \left(\frac{\partial \delta f}{\partial \phi} \right)^2 \right) + O(\delta f^3) \quad (1.83)$$

where we have dropped the bin indices for convenience. This expansion is done at each point $\vec{\xi}$ in each bin. Performing another average of this expansion and using $\langle \delta f \rangle = 0$ we have

$$\left\langle \frac{1}{f} \left(\frac{\partial f}{\partial \phi} \right)^2 \right\rangle = \frac{1}{\langle f \rangle} \left\langle \frac{\partial f}{\partial \phi} \right\rangle^2 + \frac{1}{\langle f \rangle} \left\langle \left(\frac{\partial \delta f}{\partial \phi} \right)^2 \right\rangle + \frac{1}{\langle f \rangle^3} \left\langle \frac{\partial f}{\partial \phi} \right\rangle^2 \langle \delta f^2 \rangle \quad (1.84)$$

$$- \frac{2}{\langle f \rangle^2} \left\langle \frac{\partial f}{\partial \phi} \right\rangle \left\langle \delta f \frac{\partial \delta f}{\partial \phi} \right\rangle + O(\langle \delta f^3 \rangle) \quad (1.85)$$

We can then write

$$R^2 = 1 - \left(\int d^2s \frac{1}{f} \left(\frac{\partial f}{\partial \phi} \right)^2 \right)^{-1} \sum_{i=1}^N \left(\frac{1}{\langle f \rangle_i} \left\langle \left(\frac{\partial \delta f}{\partial \phi} \right)^2 \right\rangle_i + \frac{1}{\langle f \rangle_i^3} \left\langle \frac{\partial f}{\partial \phi} \right\rangle_i^2 \langle \delta f^2 \rangle_i \right) \quad (1.86)$$

$$- \frac{2}{\langle f \rangle_i^2} \left\langle \frac{\partial f}{\partial \phi} \right\rangle_i \left\langle \delta f \frac{\partial \delta f}{\partial \phi} \right\rangle_i + O(\langle \delta f^3 \rangle) \quad (1.87)$$

The denominator in the second term is a fixed constant. The numerator however is controlled by the binning. We can therefore try to minimize this quantity.

Note that

$$\langle \delta f^2 \rangle = \langle (f - \langle f \rangle)^2 \rangle = \sigma_f^2 \quad (1.88)$$

$$\left\langle \left(\frac{\partial \delta f}{\partial \phi} \right)^2 \right\rangle = \left\langle \left(\frac{\partial f}{\partial \phi} - \left\langle \frac{\partial f}{\partial \phi} \right\rangle \right)^2 \right\rangle = \sigma_s^2 \quad (1.89)$$

$$\left\langle \delta f \frac{\partial \delta f}{\partial \phi} \right\rangle = \left\langle (f - \langle f \rangle) \left(\frac{\partial f}{\partial \phi} - \left\langle \frac{\partial f}{\partial \phi} \right\rangle \right) \right\rangle = \sigma_{fg}^2 = \frac{1}{2} \frac{\partial}{\partial \phi} \sigma_f^2 \quad (1.90)$$

where we've defined $g \equiv \partial f / \partial \phi$.

A strategy we can adopt is to attempt to minimize

$$\frac{1}{\langle f \rangle^3} \left\langle \frac{\partial f}{\partial \phi} \right\rangle^2 \sigma_f^2 + \frac{1}{\langle f \rangle} \sigma_g^2 - \frac{2}{\langle f \rangle^2} \left\langle \frac{\partial f}{\partial \phi} \right\rangle \sigma_{fg}^2 \quad (1.91)$$

for each bin. As a bonus, strategies which minimize $\sigma_f, \sigma_g, \sigma_{fg}$ will also tend to minimize higher order terms which we neglected (though this is not strictly guaranteed). This seems just about as complicated as our original problem, with the only real benefit being that we now see very intuitively that we want f and $\partial f / \partial \phi$ to be as constant as possible over each bin.

We would like to find a function, minimizing the variance of which is equivalent to minimizing the variance of (1.91). The binning technique would then be to simply create bins which are defined by intervals in that function. Any such function can be thought of as a function of f , let's call it $E(f)$. The variation of E in terms of f is

$$\delta E = E'(\langle f \rangle) \delta f \quad (1.92)$$

Note that this does not depend on any facts about variational calculus. As long as we are able to expand f away from its average in such a way that it admits a Taylor expansion at each point in phase space, $\delta E = E'(\langle f \rangle) \delta f$ will hold. Formally, what we are doing is Taylor expanding different variables at each point.

It is best to treat f and $g := \partial f / \partial \phi$ as separate. We can then write

$$\delta E = \frac{\delta E}{\delta f} \delta f + \frac{\delta E}{\delta g} \delta g \quad (1.93)$$

So

$$\delta E^2 = \left(\frac{\delta E}{\delta f} \right)^2 \delta f^2 + \left(\frac{\delta E}{\delta g} \right)^2 \delta g^2 + 2 \frac{\delta E}{\delta f} \frac{\delta E}{\delta g} \delta f \delta g \quad (1.94)$$

To get the E derivatives in terms of $\langle f \rangle$ and $\langle g \rangle$ we would have to expand them, and would get $E(\langle f \rangle, \langle g \rangle)$ plus higher order terms which we can drop.

We want to choose a function E such that minimizing the variation of that function (by choosing bins which are defined by its contours) minimizes (1.91). Sufficient conditions for such a function are

$$\frac{\delta E}{\delta f} = -\frac{g}{f^{3/2}} \quad (1.95)$$

$$\frac{\delta E}{\delta g} = \frac{1}{\sqrt{f}} \quad (1.96)$$

No choice of E satisfies both of these, however $E = g/\sqrt{f}$ satisfies both up to a constant.

Choosing bins that minimize the variance of $\frac{\partial f}{\partial \phi}/f$ or equivalently $(\frac{\partial f}{\partial \phi})^2/f$ should then minimize (1.91) and maximize R .

1.11.1 Factorization Into Slowly Varying Functions

As we will see, the method outlined above does not perform well. We believe that the reason for this is simply that in our case the function $(\frac{\partial f}{\partial \phi})^2/f$ varies so wildly (do to the sharpness of many of the resonances) that even when defining the binning by contours of this function, the result is bins in which there is a huge standard deviation of f and it's derivative such that none of the approximations of the previous section hold.

One possible way to remedy this would be to factorize $(\frac{\partial f}{\partial \phi})^2/f$ into a slowly varying part, and a part which varies wildly. The integral over the slowly varying part will than approximately cancel between the numerator and the denominator. If chosen carefully, the remaining factor may add in such a way that

it yields a result for R close to 1. To understand this, let's revisit the original binning method from [34].

Computing the expressions explicitly, we have

$$\frac{1}{f} \left(\frac{\partial f}{\partial \phi} \right)^2 = \frac{4p\bar{p}(xs - yc)^2}{p + r_B^2\bar{p} + 2\sqrt{p\bar{p}}(xc + ys)} \approx 4\bar{p}(xs - yc)^2 \quad (1.97)$$

Note that the approximation only holds in regions where $p \gtrsim \bar{p}$ (and we have used the fact that $r_B \ll 1$). However, in regions where $\bar{p} \gg p$ we obtain $(\frac{\partial f}{\partial \phi})^2/f \approx 4p(xs - yc)^2/r_B^2$, so in most cases the approximation has the same form with $\bar{p} \leftrightarrow p/r_B^2$. Likewise

$$\frac{1}{F_i} \left(\frac{\partial F_i}{\partial \phi} \right)^2 = \frac{4P_i\bar{P}_i(xs_i - yc_i)^2}{P_i + r_B^2\bar{P}_i + 2\sqrt{P_i\bar{P}_i}(xc_i + ys_i)} \approx 4\bar{P}_i(xs_i - yc_i)^2 \quad (1.98)$$

which again holds for $p \gtrsim \bar{p}$ while for $\bar{p} \gg p$ we have $\bar{P}_i \rightarrow P_i/r_B^2$. We now see that

$$R^2 \approx \frac{\sum_{i=1}^N \bar{P}_i(xs_i - yc_i)^2}{\int d^2\xi \bar{p}(xs - yc)^2} \quad (1.99)$$

This suggests a factorization method: the function $xs_i - yc_i$ cannot vary too sharply over many orders of magnitude since it is expressible in terms of trig functions. If we choose binning in which $\Delta\delta_D$ is constant, then $xs_i - yc_i$ will be approximately constant, and we will match the numerator to the denominator turn by turn. That is, they'd both be a weighted sum of $\int_i d^2\xi \bar{p}$. This is not quite true however since $s_i \neq \int_i d^2\xi s$. For simplicity, let's consider the case where $\phi = 0$. Then, to obtain $R = 1$ we'd need

$$\frac{1}{P_i} \left(\int_i d^2\xi \sqrt{p\bar{p}}s \right)^2 = \int_i d^2\xi \bar{p}s^2 \quad (1.100)$$

If s were constant over each bin we'd only need to satisfy

$$\int_i d^2\xi \sqrt{p\bar{p}} = \sqrt{P_i\bar{P}_i} \quad (1.101)$$

for perfect binning. An expansion of these expressions like the ones we did in the last section shows that this is generically closer to being satisfied than if s^2 were not constant.

Of course, the binning where c, s are constant is the binning suggested in [34]. We therefore see, in a less intuitive, but far more general way, why we'd expect this to be a good choice of binning.

1.12 Results

To test binning techniques we developed a C++ program specifically designed for this purpose. Details about the program can be found in Appendix C. The program includes modules for calculating f using a resonance model [8], generating Monte Carlo events as well as for optimizing the bin contours by various methods. As a consistency check, many of the quantities below were calculated both using numerical differentiation (with respect to ϕ) and with analytical differentiation (the latter approach requires somewhat more numerical integration). In all cases tested, the results for Q and R agreed to within two significant figures.

As a last step, in principle one should optimize the contours. That is, one should pick values of $\Delta\delta_D$ or E which define the boundaries between bins in such a way that maximizes R . This optimization presents a challenge, numerically, since the resulting function is packed with local extrema. Gradient methods therefore prove useless, and we adopted a metaheuristic method for finding global extrema (see Appendix C).

	Our result	[34] result
$N = 16$	$Q = 0.74$	$Q = 0.76$
$N = 40$	$Q = 0.76$	$Q = 0.82$

Table 1.1: Computed values for the binning quality factor Q when attempting to reproduce the results of [34], using the “ $\Delta\delta_D$ ” binning method.

	$\Delta\delta_D$	$E, (s_{13} > s_{12})$	$E, (s_{12} > s_{13})$	E (no sym)
$\phi = 0.01$	$R = 0.74$	$R = 0.69$	$R = 0.76$	$R = 0.80$
$\phi = \pi/4$	$R = 0.80$	$R = 0.60$	$R = 0.68$	$R = 0.62$
$\phi = \pi/2$	$R = 0.83$	$R = 0.31$	$R = 0.38$	$R = 0.40$

Table 1.2: Computed values of the quality factor R for binning in which the contours defining the binning have not been numerically optimized. The inequalities indicate that the bin shapes were symmetrized about $s_{12} = s_{13}$, for example $(s_{13} > s_{12})$ indicates that the bins in that region were mirrored about the line. ϕ indicates the physical value thereof.

1.12.1 Testing Previous Results

First we attempted to duplicate the results of [34] which used the same resonance model for the decay. Our result is shown in Table 1.1. This is for the “ $\Delta\delta_D$ ” binning, which is defined by contours of constant $\Delta\delta_D$.

1.12.2 Un-Optimized Results

In Table 1.2 we record some results obtained without adjusting the bin boundaries to optimize R . In the “phase binning” case (the method of [34]) this is just the “ $\Delta\delta_D$ ” binning. For our method, we choose bins defined by evenly spaced intervals in $\log((\frac{\partial f}{\partial \phi})^2/f)$. All of the following results are for $N = 16$. Here the differ-

ent variants on the E binning represent different choices for the symmetrization of the binning. Even though $(\frac{\partial f}{\partial \phi})^2/f$ is approximately symmetric about $s_{12} = s_{13}$ in most of phase space, this symmetry is certainly not exact. Therefore, if one wants symmetric binning, one can define the binning in the $s_{13} > s_{12}$ region, and then reflect those bins across $s_{12} = s_{13}$, or do the same for $s_{12} > s_{13}$. For the “no sym” result, symmetry was not enforced, however bins were still bounded by the $s_{12} = s_{13}$ line, with the same number of bins on either side. The strong dependence of our binning method on the value of ϕ is an anomaly we have still not been able to adequately explain. Note that this dependence is on the physical value of ϕ , not the value of ϕ for the function $(\frac{\partial f}{\partial \phi})^2/f$ used to define the binning (the quality in fact hardly varies at all with the latter value). One certainly expects some dependence on ϕ , but it is surprising for it to be so strong.

1.12.3 Optimized Results

The binning above was obtained by defining evenly spaced intervals in either $\Delta\delta_D$ or $(\frac{\partial f}{\partial \phi})^2/f$. This may not give the best results, and one should vary the intervals in a continuous way to find the optimum. As we mentioned previously, if R^2 is treated as a function of the interval boundary locations it is packed with local maxima. Gradient methods are therefore very difficult to use effectively. Instead we used a stochastic metaheuristic optimization method called the “Cuckoo search” [39]. This method is not very precise (although more than adequate for our purpose), but it is excellent at finding global minima. We used several different versions, with many different choices of parameter to find the best results, recorded in Table 1.3 again for $N = 16$.

	phase binning	$E, (s_{12} > s_{13})$	E (no sym)
$\phi = 0.01$	$R = 0.76$	$R = 0.77$	$R = 0.82$
$\phi = \pi/4$	$R = 0.82$	$R = 0.71$	$R = 0.64$
$\phi = \pi/2$	$R = 0.85$	$R = 0.45$	$R = 0.48$

Table 1.3: The computed value of the quality factor R for various binnings. The same as Table 1.2 but after the contours defining the bin boundaries have been numerically optimized.

1.13 Summary of Binning Improvement Results

Our binning techniques failed to best the previous method in that our binning obtained lesser values of the correct quality factor R . Recall that the binning method of [34] originally was designed to maximize Q . The previous method also had the advantage of facilitating easier extraction of s_i from D_{CP} decays, and by construction it is better for this than any other binning. We believe the poor performance of our binning is due to the fact that the probability density function f varies very sharply over many orders of magnitude, as is evidenced by the tendency of optimization to push all the bins into regions of large, positive $\log((\frac{\partial f}{\partial \phi})^2/f)$. It may then be the case that our binning has more general applicability, and may perform quite well in cases where f is more well behaved. Attempting a similar approach by factorizing $(\frac{\partial f}{\partial \phi})^2/f$ leads one back to considering the original phase binning method, since the functions c, s are natural choices for forming well-behaved factors. We have not considered the effect of experimental systematic uncertainties. Such uncertainties would have the effect of modifying $f \rightarrow \varepsilon f$ where ε is the detector efficiency as a function of s_{12}, s_{13} . Adjusting our technique to accommodate this would be trivial, but if one cannot find a technique which outperforms the phase binning, its inclusion does not seem relevant, since the effects of the more sharply varying factors will

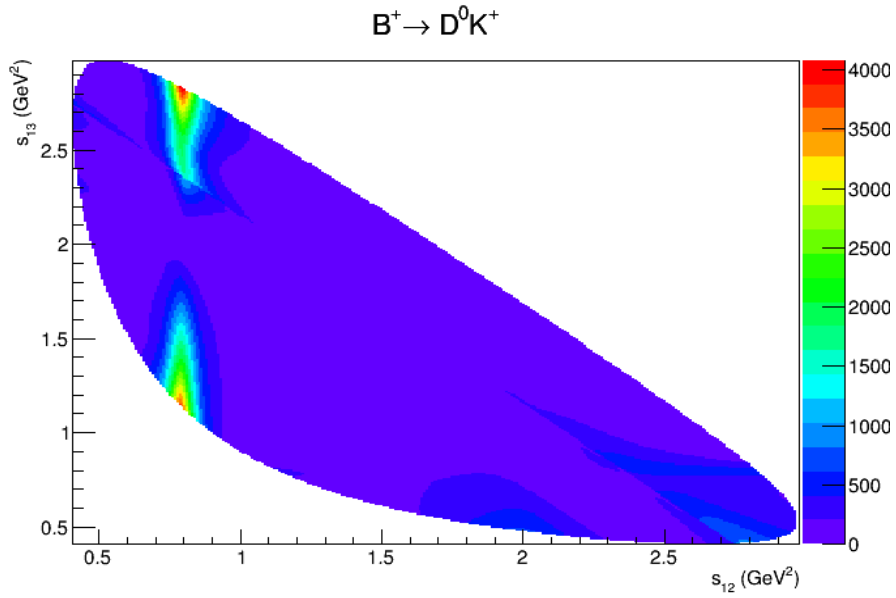


Figure 1.2: The $B^+ \rightarrow (K_S \pi^+ \pi^-)_D K^+$ amplitude (arbitrary normalization). The large peaks are both from the K_*^+ resonance. The jagged edges are a result of interference between resonances.

dominate, washing out the effects of ε except in extreme cases.

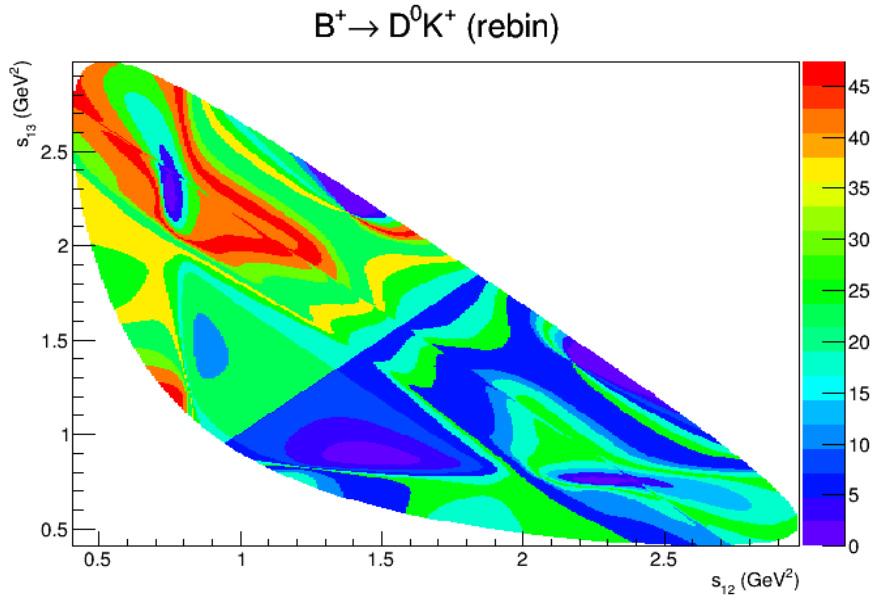


Figure 1.3: The $\Delta\delta_D$ binning for $N = 40$. The ordinate represents the integral of the $B^+ \rightarrow DK^+$ amplitude over each bin.

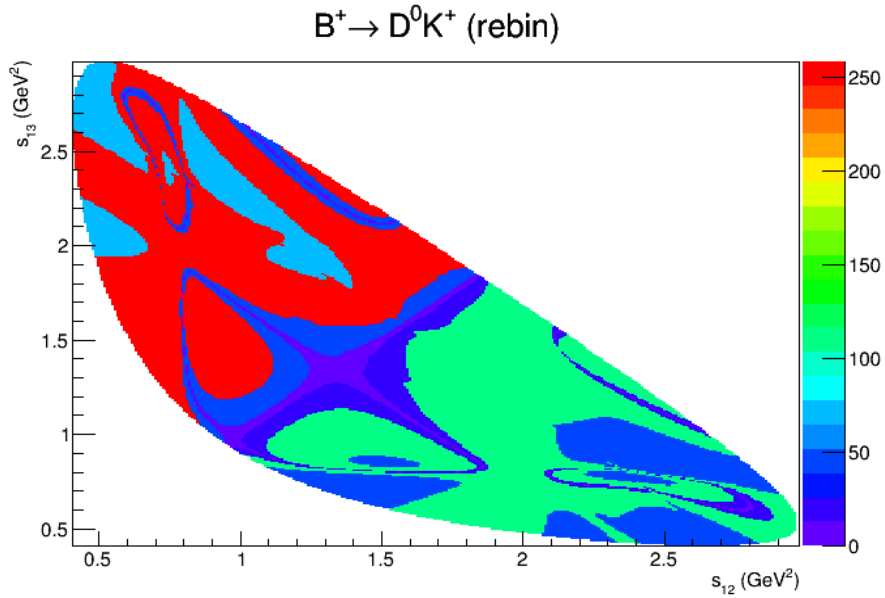


Figure 1.4: Our binning method for $\phi = \pi/4$ and $N = 16$, without imposing symmetry. The ordinate represents integrals of the decay amplitude over each bin.

CHAPTER 2
COSMOLOGICAL CONSTRAINTS ON MFV SUSY

2.1 Overview of MFV SUSY

As SUSY searches at the LHC shrink the parameter space and endanger naturalness, the need for SUSY models with radically different phenomenology becomes apparent. One way of achieving this is by relaxing the requirement of R -parity [47]. A particularly elegant way of achieving this is with MFV SUSY in which the SM Yukawas are assumed the only source of flavor and R -parity violation [50, 48, 49], enabling a triply Yukawa suppressed B and R -parity violating coupling. This coupling is trilinear in the quark superfields with the generation dependent coefficient

$$\lambda''_{ijk} = w'' V_{il}^* \epsilon_{ijkl} \frac{m_i^{(u)} m_j^{(u)} m_k^{(d)}}{v^3} \frac{1}{\sin(\beta) \cos^2(\beta)} \quad (2.1)$$

where w'' is, by assumption, an $O(1)$ parameter and $m_i^{(u)}, m_i^{(d)}$ are the up-type and down-type quark masses respectively. The indices indicate generation number. Note that for large $\tan(\beta)$ we have $\csc(\beta) \sec^2(\beta) \rightarrow \tan^2(\beta)$. The form of λ''_{ijk} is determined by demanding that the associated operator is a gauge singlet and a singlet under the $SU(3)^5$ MFV flavor group (see [51]). The resulting theory has the advantage of allowing superpartners to decay, thus evading missing energy searches, as well as evading stringent bounds from proton decay, neutron oscillations and flavor physics.

To see how the phenomenology of MFV SUSY comes about we use a spurion analysis, giving a summary of that performed in [50]. In such an analysis one considers an approximately conserved symmetry (in this case flavor symmetry)

	$SU(3)_Q$	$SU(3)_u$	$SU(3)_d$	$SU(3)_L$	$SU(3)_e$
Q	$\bar{\square}$	1	1	1	1
\bar{u}	1	\square	1	1	1
\bar{d}	1	1	\square	1	1
L	1	1	1	$\bar{\square}$	1
\bar{e}	1	1	1	1	\square
Y^u	\square	$\bar{\square}$	1	1	1
Y^d	\square	1	$\bar{\square}$	1	1
Y^e	1	1	1	\square	$\bar{\square}$

Table 2.1: The representation of the MSSM quark and lepton superfields under the $SU(3)^5$ flavor group.

to be exact, and promotes the coupling constants to fields of the appropriate representation for conserving the symmetry. We consider an $SU(3)^5$ flavor symmetry, under which each of the five quark and lepton superfields $Q, \bar{u}, \bar{d}, L, \bar{e}$ are either fundamental or anti-fundamental representations of their respective $SU(3)$. This arrangement can be seen in Table 2.1. The last three rows show the representations the SM Yukawas would need to have for the flavor symmetry to be exact. One can then ask what is the complete set of operators which are invariant under the flavor $SU(3)^5$. It turns out that in addition to the MSSM terms, there is only one additional term in the quark sector

$$W \supset \frac{1}{2} w'' (Y^u \bar{u})(Y^d \bar{d})(Y^d \bar{d}) \quad (2.2)$$

The form of the coupling λ''_{ijk} in Eq. (2.1) follows from this operator. (There is one more in the lepton sector, but its value depends on the mechanism for generating neutrino masses, and does not seem to be as good a candidate for searches.)

2.2 Introduction to Cosmological Constraints on MFV SUSY

Since MFV SUSY was formulated specifically with the intention of avoiding collider constraints, it is most often discussed in that context, whether through direct searches or flavor physics. There is a great deal of literature on the cosmological implications of R -parity violation [52, 53, 54] but none which specifically address the minimal version of MFV SUSY. (For an extension of MFV SUSY with new, stable DM candidates see [55].) Since MFV SUSY is itself so constraining (for our purposes there are essentially only two free parameters: $\tan(\beta)$ and w''), reviewing the cosmological constraints in this context is enlightening.

We find that there are two observations which provide significant constraints. The first is that any coupling which violates baryon number will rapidly bleed off existing baryon number if it is ever in thermal equilibrium, jeopardizing baryogenesis. Notably, this process is generation independent before the electroweak phase transition. As we will see this requires the baryon number violating coupling λ'' to be small as long as baryon number is generated at a temperature above the electroweak phase transition. A second important observation involves limits on dark matter decay product flux. In MFV SUSY, since the neutralino is very short lived on cosmic time scales, the most natural DM candidate is the gravitino. While gravitino production is much the same in MFV SUSY as in other SUSY models, in MFV it will decay via R -parity violating couplings. As we will see, the gravitino will be long lived on cosmic time scales, however the lifetime will nevertheless be short enough to produce a significant abundance of anti-protons and γ -rays which have not yet been observed. This would seem to imply that if MFV SUSY is a realistic model of nature and if gravitinos are to indeed play the part of DM, we should be on the verge of detecting

them indirectly.

2.3 Pedagogical Review of Baryogenesis

We will see that an important constraint on the MFV SUSY B violating coupling λ'' comes from baryogenesis. Here we pause to discuss baryogenesis more generally, for a review see, for example [41]. There is clearly a large baryon number excess in the universe: we don't usually have to worry about stepping on a pile of antimatter and being spectacularly annihilated. If there were large regions of the universe which were primarily composed of antimatter, tremendous amounts of radiation from the boundaries of such regions would be detected. The ratio of anti-proton to proton cosmic ray flux has been observed to be $\sim 10^{-4}$, while the ratio of baryon number density to entropy density $n_B/s \sim +10^{-10}$ [41]. The underlying SM Lagrangian however, would seem to have no favoritism of matter over antimatter. If baryon asymmetry were an initial condition, it would be diluted by inflation, thus making it highly fine-tuned in inflationary scenarios [44]. It is therefore often assumed that the universe evolved to its current state from one in which the local baryon number density n_B everywhere in the visible universe was exactly zero. This of course presents a problem: since baryon number appears to be strictly conserved in the SM, how can we obtain a state with large positive baryon number from one with none at all? (As we will discuss, the B symmetry in the SM is anomalous, and it may be that anomalous B violating processes called sphalerons are responsible for the baryon asymmetry.)

The solution would seem to be that there is physics beyond the standard

model in which the $U(1)_B$ baryon symmetry is violated. Indeed, based on general considerations we expect all global symmetries to be violated at the Planck scale. There are three conditions which must be satisfied in order to obtain a non-zero baryon number density from initial conditions where it is zero. These are known as the Sakharov Conditions.

- *B* Violation: This is obvious. There must be some process $X \rightarrow Y + B$ where X and Y have zero baryon number.
- *CP* Violation: In the absence of *CP* violation, the process $\bar{X} \rightarrow \bar{Y} + \bar{B}$ would have the same squared amplitude as $X \rightarrow Y + B$, thereby producing as many antibaryons as baryons.
- Loss of thermal equilibrium: In thermal equilibrium the inverse process $Y + B \rightarrow X$ happens as frequently as $X \rightarrow Y + B$, thereby producing no baryon asymmetry.

In the following sections we briefly mention three often cited baryogenesis mechanisms.

2.3.1 Electroweak Baryogenesis

As we have alluded to, the requirements of baryon number violation (through sphalerons) and *CP* violation are already present in the SM. Baryon number violation through anomalous processes is of course highly suppressed, but less so at high temperatures. The presence of these requirements for generating a baryon asymmetry in the SM has inspired the so-called electroweak baryogenesis; for a review see, for example [42].

Electroweak baryogenesis would take place during the electroweak phase transition. If the phase transition is strongly first order, it will occur through the nucleation of bubbles in the broken phase. The scattering of particles in the symmetric phase off the bubble walls can produce CP asymmetries large enough to account for the baryon asymmetry of the universe, if CP violation is present in the underlying theory. In the symmetric phase, the sphaleron B violating processes will be relatively unsuppressed, and combined with the CP violation this will produce a baryon asymmetry. As the bubble walls expand the B carrying particles will be swept into the broken phase. It is the transfer of particles from the symmetric phase where sphalerons are active to the broken phase where they are very highly suppressed (by $e^{-8\pi/g^2}$ [44]) which accounts for the out of equilibrium process, which is one of the required Sakharov conditions.

There are two major issues with electroweak baryogenesis necessitating new physics. First, the CP violation present in the SM is not sufficient to produce the required baryon asymmetry [42]. Second, it clearly requires the electroweak phase transition to be strongly first order. With the measured Higgs mass, it does not appear that this would be the case, and extensions of the SM which would produce a first order phase transition tend to clash with the measured Higgs decay phenomenology [43].

2.3.2 Leptogenesis

Another possibility is that in a complete model for neutrino masses there may be significant CP violation which somehow gets transferred to an asymmetry in baryon number. Such scenarios are referred to as leptogenesis, for reviews see

[44, 46, 45].

Here we will describe the simplest possible leptogenesis scenario. Suppose there are right-handed, sterile neutrinos which couple to the electroweak neutrinos to produce masses through the see-saw mechanism. The neutrino mass Lagrangian is then

$$\mathcal{L} \supset \lambda_{ij} \bar{L}_i H^\dagger e_{Rj} - \lambda'_{ij} \bar{L}_i H N_j - \frac{1}{2} M_{ij} \bar{N}_i N_j \quad (2.3)$$

where i, j are generation indices, and N are the right-handed neutrinos, of which there are at least two generations. In general, this sector of the Lagrangian contains CP violation (see Chapter 1). Let the heaviest of the right-handed neutrinos N_1 have mass $M_1 \gg M_i$ where the M_i are the masses of the other right-handed neutrinos. The N_1 's will be produced with a CP asymmetry. This asymmetry will then be washed out by thermal equilibrium. These heavy neutrinos will later decay, again with a CP asymmetry. If this decay occurs out of equilibrium, that is the rate of the decay process $\Gamma \ll H$, where H is the Hubble parameter, this will result in a lepton number asymmetry. If M_1 is much greater than the electroweak scale, unsuppressed sphaleron transitions will transfer the L asymmetry to B , thus creating the baryon asymmetry of the universe. Many modifications of this simple scenario exist, again see [44, 46, 45]. It will be important for us that leptogenesis necessarily occurs at a temperature far above the weak scale.

2.3.3 Affleck-Dine Baryogenesis

A slightly more exotic possibility for baryogenesis is the Affleck-Dine scenario [60]. This will hold a special significance to us since, generically, it can cause the

baryogenesis bounds we place on MFV SUSY to be evaded since it can produce the baryon asymmetry at an arbitrarily low temperature. The idea behind the Affleck-Dine mechanism is that if a scalar field carrying baryon number has a non-zero expectation value during and shortly after inflation, and its dynamics contain CP violation, it can decay to baryons with the observed abundance. The details depend strongly on things like the specific mechanism for inflation. Affleck-Dine has a tendency to produce an overabundance of baryons, but if a B carrying scalar field ϕ is initially real, the smallness of CP violating parameters in the potential is one way to keep n_B small. Good candidates for ϕ in SUSY are the flat directions. Flat directions can be found by looking for gauge singlets such as LH_u or $\bar{u}\bar{d}\bar{d}$ (so that the D terms will automatically vanish). These will be gauge neutral, but nevertheless break the SM gauge groups when they acquire a vacuum expectation value.

First consider our scalar field ϕ in the absence of interactions. Spatially homogeneous solutions satisfy

$$\ddot{\phi} + 3H\dot{\phi} + \frac{\partial V}{\partial \phi} = 0 \quad (2.4)$$

A natural choice for the interaction Lagrangian is

$$\mathcal{L} \supset \lambda|\phi|^4 + \epsilon\phi^3\phi^* + \delta\phi^4 + \text{h.c.} \quad (2.5)$$

If ϵ and δ differ by a phase, there will be CP violation. Choosing ϕ initially real, the equation of motion gives, for small ϵ, δ

$$\ddot{\phi}_i + 3H\dot{\phi}_i + m^2\phi_i \approx \text{Im}(\epsilon + \delta)\phi_r \quad (2.6)$$

for the real and imaginary parts of ϕ . Solving this and inserting into

$$n_B = \frac{1}{2i}(\phi^*\partial_0\phi - \phi\partial_0\phi^*) \quad (2.7)$$

one has

$$n_B = 2a_m \text{Im}(\epsilon + \delta) \frac{\phi_0^2}{m(mt)^2} \sin(\delta_m) \quad (2.8)$$

where a_m, δ_m are $O(1)$ numbers which parametrize the solution, and which vary depending on whether the universe is taken to be matter or radiation dominated. t is the cosmological time. So, if during inflation there are scalar fields with large expectation values which carry baryon number and their Lagrangians contain CP violation, a net baryon number asymmetry will result.

2.4 Baryogenesis Constraint on λ''

Any quantum number which is odd under CPT will be rapidly driven to zero in thermal equilibrium if it is not strictly conserved. It is therefore possible that the R -parity and baryon number violating coupling λ'' can destroy existing baryon number, potentially undoing baryogenesis. Any time the rate of the interaction mediated by λ'' is faster than the rate of the expansion of the universe it will be in equilibrium. Since by dimensional analysis this rate is $\Gamma \sim |\lambda''|^2 T$ at temperatures above the electroweak scale, and the rate of expansion is $H \sim T^2/M_p$, the rate of expansion decreases faster than the rate of interaction, so the baryon number violating interaction will be in equilibrium at late times. At the electroweak phase transition the quarks participating in the B -violating process gain masses, with the top and soon the bottom masses of the same order as the temperature so that the most dominant B -violating interactions, those with the top, fall out of equilibrium. Therefore, the rate of the B -violating process will fall off rapidly after the electroweak phase transition. It is therefore sufficient to demand that λ'' is not in equilibrium by $T \sim 100$ GeV. In [53] a Boltzmann

equation evolution of the baryon density was used to derive the constraint

$$\sqrt{\sum_{ijk} |\lambda''_{ijk}|^2} \lesssim 4 \cdot 10^{-7} \quad (2.9)$$

for squarks $m_{\tilde{q}} = 200$ GeV. Interestingly, this bound is nearly independent of the squark masses, for $m_{\tilde{q}} = 1200$ GeV the bound rises to only $5 \cdot 10^{-7}$, so this does not affect our estimate. Details including explicit Boltzmann equations can be found in [53]. Now we see that there is a stringent baryogenesis constraint on the product $w'' \tan^2(\beta)$ at large $\tan(\beta)$. Recall that w'' is a factor of the λ'' coupling which is, by assumption, $O(1)$. Note that

$$\sqrt{\sum_{ijk} |\lambda''_{ijk}|^2} \sim (2 \cdot 10^{-7}) \frac{w''}{\sin(\beta) \cos^2(\beta)} \quad (2.10)$$

This implies, for $\tan(\beta)$ not below or too close to 1

$$\tan(\beta) \lesssim \sqrt{\frac{2}{w''}} \quad (2.11)$$

For $w'' = 10^{-1}$ this implies $\tan(\beta) \lesssim 4$. This is quite significant since the requirement that the top Yukawa coupling y_t not become non-perturbatively large above the electroweak scale gives $\tan(\beta) \gtrsim 1.2$ [56]. $w'' = 1$ is therefore very nearly ruled out.

This constraint is quite important since MFV models are usually considered with large $\tan(\beta)$ to provide more realistic collider scenarios. Indeed, it puts tension on some of the most natural LSP candidates since they would then be extremely long lived. Following the estimates in [50] we have for the stop

$$\tau_{\tilde{t}} \sim (2 \text{ cm}) \frac{1}{w''^2} \left(\frac{1}{\tan(\beta)} \right)^4 \left(\frac{300 \text{ GeV}}{\tilde{m}_t} \right) \quad (2.12)$$

for the left-handed sbottom

$$\tau_{\tilde{b}_L} \sim (41 \text{ m}) \frac{1}{w''^2} \left(\frac{1}{\tan(\beta)} \right)^6 \left(\frac{300 \text{ GeV}}{\tilde{m}_{b_L}} \right) \quad (2.13)$$

and for the neutralino

$$\tau_{\tilde{N}} \sim (2 \text{ m}) \frac{1}{w''^2} \left(\frac{1}{\tan(\beta)} \right)^4 \left(\frac{300 \text{ GeV}}{m_{\tilde{N}}} \right) \quad (2.14)$$

As we see, the sbottom is ruled out as an NLSP for small $\tan(\beta)$ (the exclusion comes from heavy stable charged particle (HSCP) searches [57, 58]) while the neutralino is marginal. Requiring that the stop decays within 5 m so that it is too short lived to travel all the way through the muon arms of CMS and ATLAS and has a chance of evading HSCP searches we have

$$\tan(\beta) \gtrsim \frac{1}{4} \sqrt{\frac{1}{w''}} \left(\frac{300 \text{ GeV}}{\tilde{m}_t} \right)^{1/4} \quad (2.15)$$

Even for $w'' = 10^{-1}$ (which gives $\tan(\beta) \gtrsim 3/4$) this bound is weaker than that from the perturbativity requirement on y_t , but as we will see it may be significant for very low w'' which baryogenesis and DM constraints force us to consider. For example, for $w'' = 10^{-2}$ we have $\tan(\beta) \gtrsim 2.5$. Recall also that the left hand side of (2.15) should be replaced with $\sqrt{\csc(\beta) \sec^2(\beta)}$ for $\tan(\beta) \lesssim 1$. Later (see Fig. 2.3) we will review this in relation to cosmological constraints.

Of course, the baryogenesis constraint can be avoided either in part or entirely in any scenario in which baryon number is generated at or below the electroweak phase transition. There would likely be some constraint on λ'' in electroweak baryogenesis since baryon number is still generated in the symmetric phase, but we expect it to be much weaker. (Electroweak baryogenesis may have its own implications on $\tan(\beta)$, see [59].) Scenarios with arbitrarily low reheat temperature such as Affleck-Dine baryogenesis (for a review see [60]) evade this constraint entirely. If inflation happens at GUT scales, it is much more difficult to achieve very low reheat temperatures so that our baryogenesis constraint is harder to avoid using Affleck-Dine. In other scenarios in

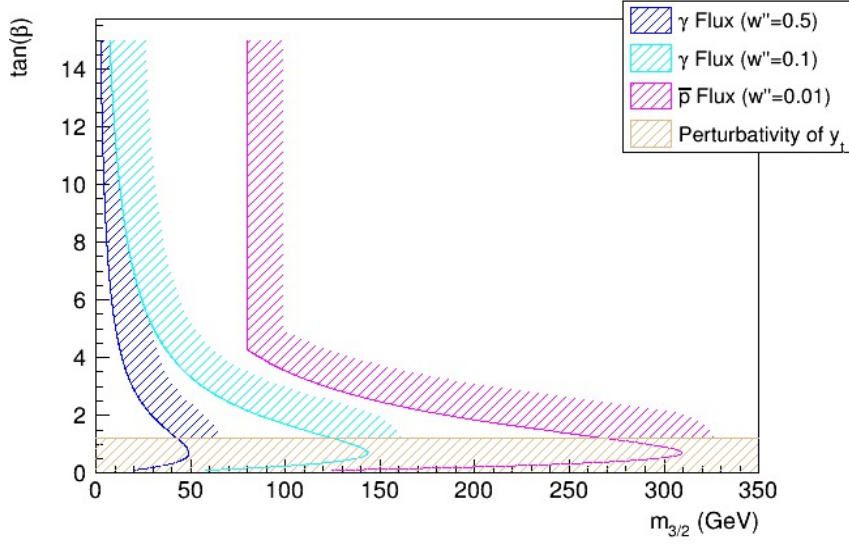


Figure 2.1: Upper limit on the gravitino mass as a function of $\tan(\beta)$ in order for it not to produce excessive \bar{p} or γ flux. Excluded regions are on the sides of the solid lines with hashing. The reason for the hard cutoff at $m_{3/2} = m_W$ in the $w'' = 0.01$ line is because the \bar{p} flux constraint is based on $\tilde{G} \rightarrow W^\pm \ell^\mp$.

which baryon number is generated above the electroweak phase transition such as thermal leptogenesis, this constraint remains quite severe.

2.5 Gravitino DM in MFV SUSY

In MFV SUSY gravitinos are unstable, and if they are the LSP and lighter than the top they decay predominantly through the channel $\tilde{G} \rightarrow cbs$ with lifetime

$$\tau_{3/2} \sim (2 \cdot 10^{25} \text{ s}) \frac{1}{w''^2} \left(\frac{100 \text{ GeV}}{m_{3/2}} \right)^3 \sin^2(\beta) \cos^4(\beta) \quad (2.16)$$

(For a review on gravitino coupling to matter, see, for example [61].) Again, for large $\tan(\beta)$, $\sin^2(\beta) \cos^4(\beta) \rightarrow \tan^{-4}(\beta)$. Note that if the gravitino is heavier than

	<i>cbs</i>	$Z\nu$	$W^\pm\ell^\mp$
$p + \bar{p}$ multiplicity	1.9	1.5 (1.7)	1.5 (1.6)

Table 2.2: Multiplicities of protons or anti-protons for the final state relevant to MFV (*cbs*) and two others, from Pythia 8, for 100 GeV gravitinos. In parentheses are multiplicities reported by [63] to which we compare. We attribute the difference to the different versions of Pythia being used. We find that these values are nearly independent of the gravitino mass in the range of interest.

the top, it will not be sufficiently long-lived to be a DM candidate in MFV SUSY. While our estimate of $\tau_{3/2}$ is indeed much longer than the age of the universe, it will lead to a significant excess of cosmic rays. Note that since *cbs* has baryon number $|B| = 1$, the ultimate final state will necessarily contain at least one proton or anti-proton. There will also be a significant number of photons produced in the Dalitz decays of neutral pions.

2.5.1 Anti-proton Constraints from PAMELA

The PAMELA experiment reports no statistically significant excess of anti-protons in the range 60 MeV to 180 GeV after 850 days of running [62]. A number of analyses have been carried out to derive lower limits on gravitino DM lifetime based on this data [64, 65, 63, 66], some of which study RPV scenarios, though not for the decay mode $\tilde{G} \rightarrow cbs$. Unfortunately these bounds suffer from enormous uncertainties of several orders of magnitude (in seconds) due to astrophysical effects on the propagation of anti-protons through the galaxy as well as astrophysical background and uncertainty in the shape of the galactic DM halo profile. For extreme values of astrophysical parameters, all these anal-

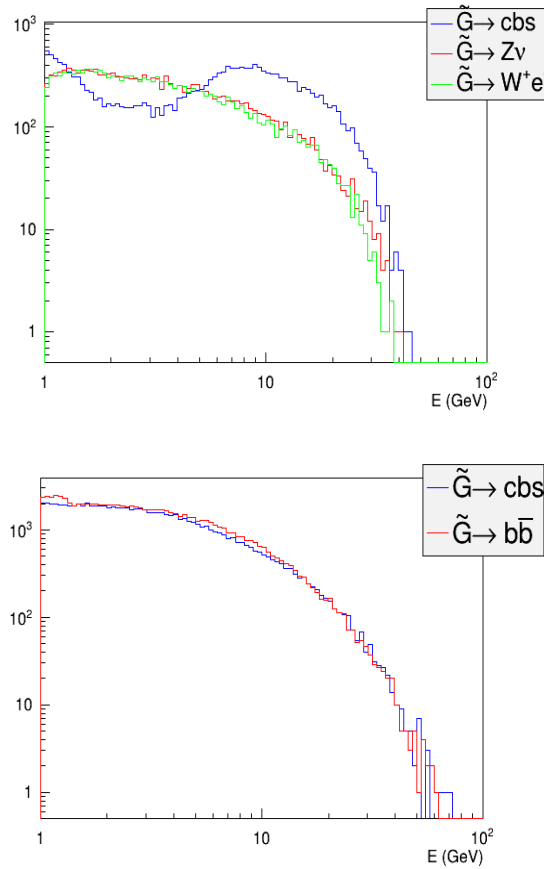


Figure 2.2: Comparison of anti-proton (left) and photon (right) spectra for various different final states generated using Pythia 8 and $m_{3/2} = 100$ GeV. The ordinate shows the number of particles, where 10^4 events were generated for each case. The shapes of the spectra were found to depend weakly on the gravitino mass in the region of interest (down to about m_W for anti-protons and about 20 GeV for photons).

yses conclude a lower limit of no less than 10^{26} s for the DM lifetime with masses in the range m_W to about m_t (unfortunately these do not consider very low, order GeV gravitino masses due to the final states being considered, though we will see that the resulting bounds force us into this region). Though they consider different decay modes, the cbs final state has a similar $p + \bar{p}$ multiplicity to those studied (see Table 2.2). For example [63] considers $W\ell$ and $Z\nu$ final states with

$p + \bar{p}$ multiplicities each of about 1.6, and concludes a lower limit on the lifetime of about $2 \cdot 10^{27}$ s for 100 GeV gravitinos (and roughly similar values up to the top mass). We used simulations in Pythia 8 [67] to conclude that in our case the anti-proton multiplicities and spectra are similar to the analysis of [63] (see Fig. 2.2). One should note that the PAMELA data is most constraining in the range from a few GeV through a few times 10 GeV. There is a dip in the $\tilde{G} \rightarrow cbs$ anti-proton spectrum around 2 GeV, but it is greater than the $\tilde{G} \rightarrow Z\nu(W^\pm e^\mp)$ spectra above about 10 GeV. We can therefore repurpose the $\tilde{G} \rightarrow Z\nu$ and $\tilde{G} \rightarrow W^\pm e^\mp$ analyses to conclude that it would place a lower limit on the $\tilde{G} \rightarrow cbs$ lifetime of about

$$\tau_{3/2} \gtrsim 10^{27} \text{ s}, \quad (2.17)$$

restricting us to a rather uncomfortable region of MFV SUSY parameter space. While one can increase the lifetime to about 10^{27} s by taking $w'' \sim 0.1$ for $\tan(\beta) \approx 1$, in doing so one starts to create tension with collider data since the NLSP's may become so long-lived as to be excluded by missing energy or direct searches as can be seen in Eqs. (2.12,2.13,2.14). This lifetime limit gives us a constraint on $w'' \tan^2(\beta)$ for $\tan(\beta) \gtrsim 1$

$$\tan(\beta) \lesssim \frac{0.4}{\sqrt{w''}} \left(\frac{100 \text{ GeV}}{m_{3/2}} \right)^{3/4} \quad (2.18)$$

In Fig. 2.1 we plot upper limits on $m_{3/2}$ as a function of $\tan(\beta)$ derived from (2.17).

2.5.2 γ -Ray Constraints from Fermi LAT

Simpler analyses are carried out searching for an excess of high energy cosmic photons due to dark matter decay or annihilation, most recently from Fermi LAT [68, 69, 70]. Even in these cases it is not quite so simple to compare with

	<i>cbs</i>	<i>b\bar{b}</i>
γ multiplicity	15.7	16.7

Table 2.3: Comparison of multiplicities of final state photons from *cbs* and from *b \bar{b}* as determined from Pythia 8 for 100 GeV gravitinos. Again, we find these values to be approximately independent of $m_{3/2}$ in the region of interest (for $m_{3/2} = 20$ GeV we have the *cbs* and *b \bar{b}* multiplicities at about 8 and 13 respectively).

	<i>cbs</i>	$Z\nu$	$W^\mp e^\pm$
$e^+ + e^-$ multiplicity	0.48	0.44	1.39

Table 2.4: Comparison of multiplicities of final state electrons and positrons from *cbs*, $Z\nu$ and $W^\pm e^\mp$, found generating 10^4 events in Pythia 8 with $m_{3/2} = 100$ GeV.

the predicted flux because of the details of the data selection (a glance at our references will reveal that this can still be the cause of significant uncertainty), however we can still take advantage of lifetime limits concluded from these analyses.

We compare photons produced in $\tilde{G} \rightarrow cbs$ to those produced in $\tilde{G} \rightarrow b\bar{b}$ as in [69]. Using Pythia 8 we find that the photon multiplicities of these final states are similar (see Table 2.3). We also find that the spectra of photons in these cases are very nearly identical (see Fig. 2.2). From this and [69] we can conclude the somewhat weaker bound

$$\tau_{3/2} \gtrsim 10^{26} \text{ s} \tag{2.19}$$

2.5.3 PAMELA e^+ Excess

We should briefly mention that MFV SUSY gravitinos cannot explain the PAMELA and AMS positron excess [71, 72]. An analysis has been carried out showing that gravitino decay to $Z\nu$ or $W^\pm e^\mp$ can explain this excess [73]. While these final states have similar overall positron multiplicities to $cb\bar{s}$ (see Table 2.5.3), both $Z\nu$ and $W^\pm e^\mp$ exhibit a sharp rise in their spectra around a few tens of GeV (for $100 \text{ GeV} \leq m_{3/2} \leq 200 \text{ GeV}$). More importantly it can be seen in [73] that gravitino masses at least as large as the top mass are needed to explain the entire excess, while also requiring $\tau_{3/2} \sim 10^{26} \text{ s}$, which is essentially ruled out in this model by the absence of an anti-proton excess.

2.6 Summary of Cosmological Constraints on MFV SUSY

We have seen that cosmological evidence combined with the requirement that the NLSP not be too long lived severely constrains MFV SUSY, at least in the most orthodox models of reheating and baryogenesis. These constraints are shown on the $(w'', \tan(\beta))$ parameter space in Fig. 2.3. This combined with flavor physics constraints [74, 75] would seem to strongly suggest that $\tan(\beta)$ must be small even for MFV SUSY, and it is pushed uncomfortably close to saturating the limit $\tan(\beta) \gtrsim 1.2$, which is required for the top Yukawa y_t to remain perturbative. If the gravitino DM scenario is to be believed, then combined with baryogenesis considerations it is certainly true that λ'' must be significantly smaller than its upper limit based on proton decay and flavor physics alone. The gravitino is still a DM candidate, since there is no obstacle in making $m_{3/2}$ as low as 10 GeV in order to avoid constraints from indirect detection, but to do so one must be

willing to accept a reheating temperature of no more than about 10^7 GeV, which would be problematic for thermal leptogenesis. The cosmological constraints we have considered here suggest a lower gravitino mass than is often recently studied.

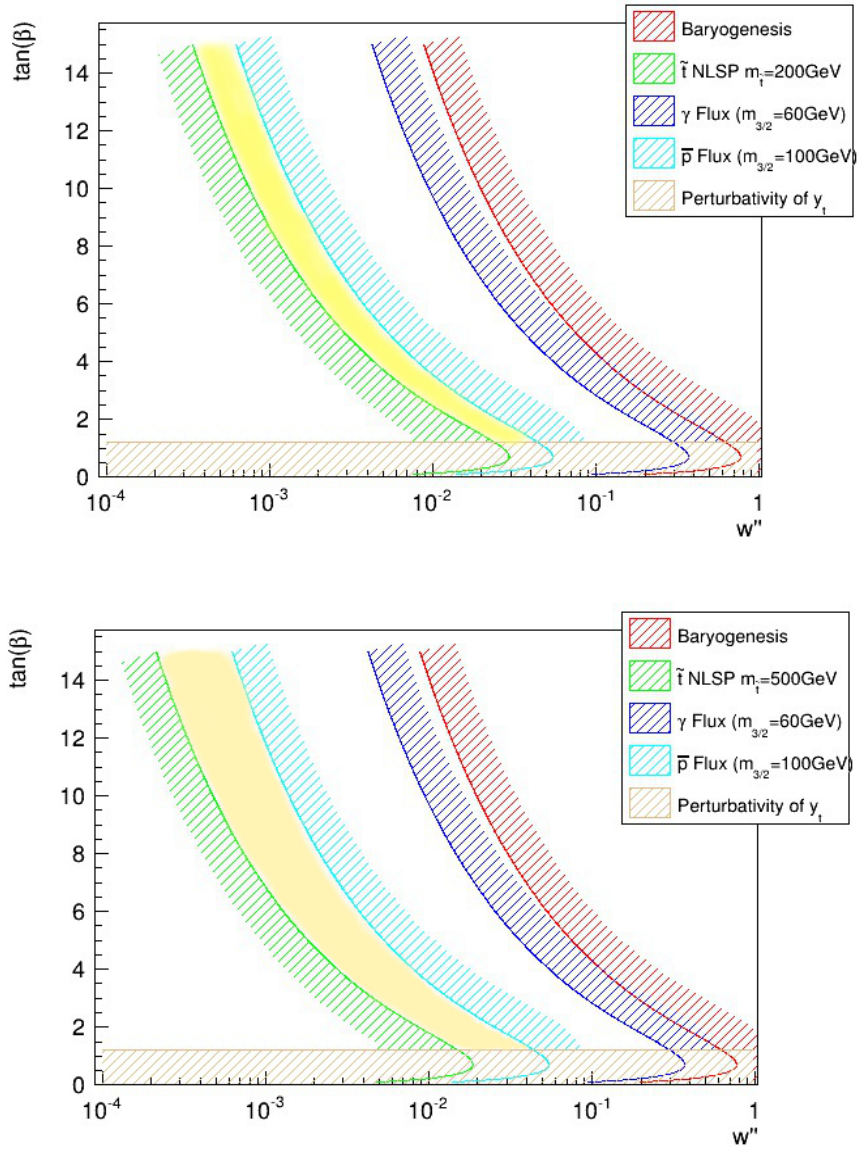


Figure 2.3: Constraints on the MFV SUSY parameter space due to cosmological considerations. Excluded regions are on the sides of the lines with hashing. The region allowed by all constraints is highlighted in yellow. We show a possible bound from below assuming the \tilde{t} is the NLSP and requiring it not live more than 5 m so that it would not have been detected as a heavy stable charged particle at the LHC for two different values of $m_{\tilde{t}_1}$. (The limit of 5 m is taken so large in order to account for the possibility of low-velocity stops and is thought to be quite conservative.)

CHAPTER 3
THE FATE OF ORBITALLY EXCITED DARK MATTER

3.1 Strongly-Interacting Dark Matter with Excited States

The non-discovery of weakly interacting massive particles (WIMP) through direct collider searches has motivated interest in more exotic models for Dark Matter (DM), in particular, models in which the DM particles have their own complicated dynamics [78, 76, 77, 80, 79]. Of specific interest to us are models where the DM self interaction is strong and confining, in a way similar QCD. These strong dynamics provide ways to stabilize the DM that are absent for weakly coupled theories.

In this chapter we investigate a particular model where the quarks of the DM sector are much heavier than its confinement scale. For simplicity we consider $SU(N)$ gauge groups with matter fields in the fundamental representation, which we call quarks. In such models the quarks will hadronize into a charmonium-like state, that is, a bound state of two heavy quarks. Such states can be very long lived if they have large angular momentum. Unlike in QCD, there are no light pions to emit in order to shed the angular momentum, and in these states the wavefunction overlap at the origin is zero, so the annihilation probability is suppressed.

While such a mechanism is intriguing and looks promising, we find that it cannot stabilize these states over cosmological time scales. There are three model independent reasons for this. First, there is an upper bound on the orbital excitation of bound states beyond which they will decay strongly to glue-

balls of the hidden $SU(N)$. This in general prevents one from considering stable bound states of $L \gtrsim 10$, placing an upper bound on the centripetal suppression of annihilation amplitudes. This is discussed in Section 3.3. Second, as we discuss in Section 3.5, we recall the fact that states with non-zero angular momentum have their annihilation amplitude suppressed by roughly α^L . For strongly coupled systems we cannot have $\alpha \ll 10^{-1}$, so even orbitally excited states are indeed quite short lived on cosmic timescales. Finally, if there exist stable excited states they can de-excite through semi-elastic collisions with each other. We find that if this process occurs, it will continue until it freezes out (an event we call the “second freezeout”). At this time there are essentially no excited states remaining, even if they are stable. This is discussed in Section 3.4. In the appendices we include expressions useful for performing detailed model specific calculations.

3.2 The model, notations and scales

As stated in the introduction, most of our considerations apply to a wide class of models. Additionally, some sections are applicable to models which others are not. We will defer to the readers judgment in these matters, since it is not our task here to enumerate specific models and their consequences. For the sake of concreteness, one should think of the simple model presented in this section, but be aware that most of our results have more general applicability.

We consider a model with a gauged $SU(N)$. We assume that the $SU(N)$ symmetry is confining with anomalous dimension Λ . We include one matter field, denoted as χ , in the fundamental. We call this field a dark quark or simply a

quark. χ can be a scalar or a fermion, and we do not specify which. Our notation for the anti-particle will be $\bar{\chi}$. We denote the mass of the dark quark by m_χ , and we further assume that $m_\chi \gg \Lambda$. We denote the dark gluon as g_D .

The spectrum of the hidden sector consists of gluballs and a quarkonia-like state. We discuss the details of the spectrum later, here we just mention that the lightest state is the lightest glueball. As for the notation, we denote a generic glueball as G , and specific ones as G_i . We denote a general quarkonia-like state as ψ , and specific ones with ψ_i . (In both cases the subindex are sorted by the mass, that is, $m_i > m_j$ for $i > j$.) When we care about the spin of the state, we may denote it by ψ^J .

We consider the case where the couplings between the new sector and the SM are very small. In particular, we assume a Z_2 symmetry that forbids χ to decay to SM particles, and thus, the only interaction between the two sectors is via pair annihilation and creations. We parametrize the coupling to the SM fields as

$$\epsilon \equiv \sigma(\chi + \bar{\chi} \rightarrow X_{\text{SM}})\sigma(\chi + \bar{\chi} \rightarrow g_D g_D), \quad (3.1)$$

where X_{SM} is a final state made up of SM particles, and we sum over all of them. While in principle ϵ is a function of q^2 we assume that the underlying process is mediated by heavy states and thus the q^2 dependence is small and we neglect it.

In addition to those above we require some cosmology-related definitions. First we define

$$X_i = \frac{n_i}{N}, \quad N = \sum_i n_i \quad (3.2)$$

where n_i is the number density of the i th bound state particle. We will also define a as the cosmological scale factor and $H \equiv \dot{a}/a$ is the Hubble parameter.

With these definitions we can discuss the relevant scales that are important in our study. We assume that we start in a situation where the temperature $T \gg m_\chi$, the universe is in a plasma without confinement, and the χ s are in thermal equilibrium. The first scale we encounter is the temperature scale at which there is separation between the SM and the dark sector, that is when

$$\chi\bar{\chi} \rightarrow X_{\text{SM}}, \quad \text{and} \quad g_D g_D \rightarrow X_{\text{SM}} \quad (3.3)$$

drop out of equilibrium. We call this event the “first freezeout” and denote its temperature by T_{1f} the this separation occurs (the reason we called it the “first” will become clear shortly). The value of T_{1f} depends on the details of how the dark sector is coupled to the standard model, for an introduction see [96]. If, for instance, the dark matter is coupled to the standard model via a gauge boson such that its annihilation to SM cross-section is $\sigma \sim \alpha^2/T^2$

$$T_{1f} \sim \alpha^2 M_{\text{Pl}} \quad (3.4)$$

Since our analysis does not depend on the specific value of T_{1f} , we treat it as a free variable, with the only constraint being that $T_{1f} \gg \Lambda$.

Note that after T_{1f} the temperature of the SM and the dark sector are not the same. In the following, unless specifically stated otherwise, when we refer to temperature we are referring to the temperature of the dark sector.

After the annihilations to SM content has ceased, at some point the dark gauge sector will undergo a phase transition to the ψ_i bound states. As in QCD, this occurs for $T \sim \Lambda$. It is vital for our discussion to apply that this phase transition occurs, and that there is a significant remaining number density of the ψ_i bound states. None of our discussion can apply to models where, for instance, the dark sector is so dilute before Λ that the dark quarks and gluons effectively decouple before the phase transition.

The mass density changes very little during the phase transition. An important point to make is that we expect that a significant fraction of the bound states that are formed are excited states. While we cannot prove it, this is the general expectation, since there is no reason to believe that any two particles will encounter each other without relative angular momentum. Moreover, this is, again, a conservative assumption, if the angular momentum was small to start with the states would annihilate fast, and they will not be able to be DM candidates.

Our final assumption is that after confinement the ψ states interact with each other via a semi-elastic interaction

$$\psi_i \psi_j \rightarrow \psi_k \psi_l + E. \quad (3.5)$$

Later on, when the temperature drops even further, the above interaction also passes out of equilibrium. We denote that event as “the second freezeout” and denote its temperature by T_{2f} . After the second freezeout the only way of changing the number density of ψ is via internal annihilation, $\psi \rightarrow GG$.

Thus, the model we are investigating is one where we assume that $m_\chi \gg \Lambda$ and there is a mechanism where the dark matter forms bound states. In the following we see how these states evolve and show that they cannot persist over cosmically significant timescales.

3.3 Instability of highly excited states

After the phase transition to confinement, the states ψ_i with $i \gg 1$ will decay strongly via $\psi_i \rightarrow \psi_j + G$ with $i > j$. This is because for large enough i the

differences in masses $M_i - M_1$ is greater than the mass of the lightest glueball. We know that the glueball mass depends linearly on Λ , but only weakly on other parameters, such as the gauge group or the heavy quark content. Thus, we expect the lightest glueballs to have masses $O(7\Lambda)$ [88, 89]. Since the mass splitting between L states in mesons is $O(\Lambda)$ [87] we expect those states with $L \gtrsim 7$ to be unstable against strong decays. In QCD, charmonium is the best known spectrum and states above $1D$ have not been identified [90]. The difference in masses between these and the ground state is less than the mass of the lightest glueball, so in a world without pions they would be absolutely stable.

The spectrum of the theory we are considering depends crucially on the ratio

$$r \equiv \frac{m}{\Lambda}. \quad (3.6)$$

We model the potential as

$$V = \frac{-\alpha}{r} + \sigma r \quad (3.7)$$

where $\alpha = \alpha(m)$ and is small and σ encode the confining interaction. In general we expect $\sigma \sim 4\Lambda$ [99].

For $\sigma = 0$ we get a system similar to a hydrogen atom, while for large σ we have a spectrum that looks more like QCD. The transition between these two regions can be estimated thus

$$\sigma r \sim \alpha/r \rightarrow r^2 \sim \alpha/\sigma \sim \alpha/4\Lambda. \quad (3.8)$$

At what n do we get this r ? In the $1/r$ case we know that $r \sim n^2/(\alpha m)$. We then conclude that for

$$n^2 < \frac{\alpha^{3/2} m}{4\Lambda} \quad (3.9)$$

we can use the Coulomb potential results. For Larger n the linear confining potential is the dominant one. Assuming no angular momentum, we can ap-

proximate the result of the linear potential

$$E_n = -c_n \left(\frac{\sigma^2}{2m} \right)^{1/3} \quad (3.10)$$

where c_n are the zeroth on the Airy function (and recall that they are all in $x < 0$).

We now consider what states are stable against decay by glueball emission. In the case the Coulomb potential is valid for the first few states we know that

$$\Delta E \geq \frac{3}{4} \frac{m\alpha^2}{4} = \frac{3m\alpha^2}{16} \quad (3.11)$$

(The formula for the Hydrogen atom has $\mu/2$ but for us $\mu = m/2$.) The glueball mass is about 7Λ . Thus as long as

$$\frac{\Lambda}{m} \lesssim \frac{3\alpha^2}{112} \quad (3.12)$$

all the excited states can decay to the ground state.

In the other limit, we can have a situation where many states are stable against radiative decays. Using (3.9) we learn that the Coulomb approximation is valid when

$$n^2 \lesssim \frac{\alpha^{3/2} m}{4 \Lambda} \quad (3.13)$$

Thus, for some region of parameter space we can have many states that are stable against radiative decays.

In the linear potential case the spacing is close to constant (a constant spacing is achieved in the case of an harmonic potential). Yet, a typical spacing is of order $(\sigma^2/m)^{1/3}$, and thus the number of states that we have that are stable is of order $(7\Lambda)/(\sigma^2/m)^{1/3}$

Last we need to discuss the lifetime of the states that can decay. It is well known that for a Coulomb potential the Rydberg states can have lifetimes that

are much longer than the lowest states. The reason is essentially phase space to decay to nearby states. In our case this effect is not as important the linear terms becoming important, and the spacing getting bigger. Thus, we expect all of the decay to occur rather fast without any phase space suppression.

3.4 Collisional De-excitation of Orbitally Excited States

Once the bound states have de-excited sufficiently that they can no longer emit glueballs, there are still ways for them to lose energy and change their angular momentum through collisions like the one in Eq. (3.5). Here we estimate the range of temperatures at which this process is likely to occur and what will be the abundance of final states once it has ceased.

A first-principles treatment of the interaction underlying the collisional de-excitation of pairs of two-body bound states is extremely formidable since it involves non-perturbative strong dynamics in a four body problem. We can, however, estimate the effect using a simple geometric cross-section. While this is clearly not going to give us exact results, it should provide a reliable order of magnitude estimate.

The interaction we are considering is given in Eq. (3.5). We consider this for sufficiently small kinetic energies such that $T \ll \Lambda$. If this relation is not satisfied, fully inelastic collisions would dominate, necessitating a more sophisticated treatment. In our case, since the excited states are stable against radiating glueballs or other light states, there cannot be additional particles in the final state. Instead, all of the energy from the de-excitations must be manifest as kinetic energy of the final state particles. Note that re-excitations in this regime

are highly suppressed by the assumption that the temperature is low.

In this scenario the momentum dependence of the cross-section is very weak as the relevant partial wave expansion is p/Λ . Thus, we can only consider s -wave scattering and we use as an approximation a geometric cross section, $\sigma_{tot} \sim 1/\Lambda^2$. See Appendix B.3.

The thermal average cross-section $\langle\sigma v\rangle$ is defined in the usual way in Appendix B.2 (also see [96]). We consider a simplified case where the initial particles have the same mass, M , and get

$$\langle\sigma v\rangle = \frac{1}{2J+1} \frac{16\sqrt{\pi}}{\Lambda^2} \sqrt{\frac{T}{M}} \quad (3.14)$$

The pre-factor of $1/(2J+1)$ reflects the fact that only s -wave interactions are included.

It is straightforward to find $\langle\sigma v\rangle$ for particles of different masses, but the result is a complicated expression in terms of error functions. We expect to be of the same order of magnitude. The T dependence of $\langle\sigma v\rangle$ is the same as for the same mass case long as the cross-section is momentum independent. Similarly, we expect the dependence on the final state masses to be weak. See Appendix B.2 for more details.

Now we are ready to write Boltzmann equations appropriate for our case. The relevant Boltzmann equations are derived in Appendix B.1

$$\frac{d\log(X_i)}{d\log(a)} = -\frac{N}{H} \left(\frac{1}{X_i} \sum_{k,l} \alpha_{kl} X_k X_l \right) \quad (3.15)$$

Another useful way of writing the same equation is

$$\frac{d\log(X_i)}{d\log(T)} = T \frac{\Lambda^2(N_f/T_f^3)}{H_1} \left(\frac{1}{X_i} \sum_{k,l} \alpha_{kl} X_k X_l \right) \quad (3.16)$$

where $H_1 = H(T = \Lambda)$ and N_f, T_f are the total number density and temperature at the $SU(N)$ phase transition (so that $T_f \sim \Lambda$). The α 's are simply thermal average cross-sections but they should be selected judiciously. For example, in a two state system $i \in \{0, 1\}$, one has

$$\frac{d \log(X_1)}{d \log(a)} = -\frac{N}{H} \frac{1}{X_1} (\alpha_{11} X_1^2 + \alpha_{10} X_1 X_0) \quad (3.17)$$

where $\alpha_{11} = 2\langle\sigma v\rangle(11 \rightarrow 00) + \langle\sigma v\rangle(11 \rightarrow 01)$ and $\alpha_{10} = \langle\sigma v\rangle(10 \rightarrow 00)$, see Appendix B.1.

From (3.15) we see that collisional de-excitation will cease and the relative abundances will reach steady state when $\Gamma = N\langle\sigma v\rangle \sim H$ (assuming the thermal average cross-sections are all of the same order). We can therefore estimate this temperature, which we call the temperature of the second freezeout T_{2f} , just as we would estimate the freezeout temperature of DM annihilation. Assuming the mass of the DM particles are all of the same order we have

$$N \sim \frac{\rho_{DM}}{M} = \frac{\rho_{DM0}}{M} \left(\frac{T}{T_0}\right)^3 = \frac{1}{M} \Omega_{DM0} \rho_{crit0} \left(\frac{T}{T_0}\right)^3 \quad (3.18)$$

where a subscript 0 denotes a present-day value (simply a useful reference point for which various parameters are well-known) and $\rho_{crit} = 3H^2 M_p^2 / 8\pi$ is the critical density. Assuming the second freezeout occurs during radiation domination, from $\Gamma \sim H$ we have

$$\frac{1}{M} \Omega_{DM0} \rho_{crit0} \frac{T_{2f}^3}{T_0^3} \frac{1}{\Lambda^2} \sqrt{\frac{T_{2f}}{M}} \sim \frac{T_{2f}^2}{M_p} \quad (3.19)$$

Using that $\Omega_{DM0} \sim 1$ we can estimate the temperature

$$T_{2f} \sim M \left(\frac{\Lambda^2 T_0^3}{M_p^3 H_0^2} \right)^{2/3} = 10^{-6} M \left(\frac{\Lambda}{1 \text{ GeV}} \right)^{4/3} \quad (3.20)$$

At temperatures lower than this, elastic and semi-elastic collisions between DM particles no longer take place. We assume the collisional de-excitation can take place as long as collisions are relevant.

In most models we require $\Lambda \ll 1 \text{ GeV}$ so that the hidden sector does not over-close the universe [77], however in general M can be quite large (owing to the mass of the constituents of course). Therefore, T_{2f} can vary wildly depending on the specific model. For example, if $M = 1 \text{ TeV}$ and $\Lambda = 1 \text{ eV}$ then the second freezeout has not even occurred yet, however for $M = 100 \text{ TeV}$, $\Lambda = 1 \text{ MeV}$ the second freezeout occurs not long after nucleosynthesis.

3.4.1 Reheating through Collisional De-excitation

Even though the number density of DM particles for $T \ll \Lambda$ is much lower than at the phase transition, a comparatively huge amount of energy, specifically Λ per collision, can be injected into the DM gas through collisional de-excitation. If the energy is too large, (3.15) will contain a mixture of terms for elastic, semi-elastic and inelastic hard scattering, the latter of which will require a full-blown quantum field theory with a specific model to consider. This may also be the case when $T \sim \Lambda$ depending on the details of the $SU(N)$ phase transition. The details of what happens during such a “reheating” period are beyond the purview of this dissertation. To prevent this from happening, we require the rate at which energy is injected through interactions is much lower than the rate of energy loss through cooling from expansion, which leads to

$$\left(\frac{T}{M}\right)^{3/2} \ll \left(\frac{M\Lambda}{10^9 \text{ GeV}^2}\right) \quad (3.21)$$

(see Appendix D). If this condition is satisfied for all $T < \Lambda$, this sort of reheating will never occur. If not, presumably hard inelastic interactions will be important until the temperature is sufficiently low that (3.21) is satisfied and semi-elastic collisional de-excitation again dominates. (See Appendix D for more detail.)

3.4.2 Relic Density of Excited States

As one may guess, it turns out that there are essentially no excited states left by the temperature T_{2f} . This is not quite a trivial matter however, since it may be that T_{2f} is reached while there is still a significant fractional abundance of excited states. To compute the relic abundance of excited states one should numerically solve the full Boltzmann equations (3.15) for a specific model.

To get a rough estimate, we consider a two-level system, defining $\chi \equiv n_1/n_0$. Since the cross-sections involved are all of the same order, this will give us a general idea of the behavior of a system with more possible excitations, where we can think of n_1 as being the number density of the most excited half of states, and n_0 as being the number density of the least excited half of states. When we find that $\chi(T \rightarrow 0) \ll 1$ this indicates that at least the top few most excited states will have low abundance in n -level systems.

As derived in Appendix B.1 we have the Boltzmann equation

$$\frac{d\chi}{dy} = \frac{N_f \langle \sigma v \rangle}{H_1} (2\chi^2 + f\chi) \quad (3.22)$$

where $\chi \equiv n_1/n_0$, $y \equiv T/\Lambda$ and N_f is the DM number density at $T = \Lambda$. f is an $O(1)$ fudge factor accounting for the difference in $1+1 \rightarrow 0+0$ and $1+0 \rightarrow 0+0$ cross-sections (really it depends weakly on T , see Appendix B). We write $\langle \sigma v \rangle = \langle \sigma v \rangle_0 \sqrt{\Lambda y/M}$. Integrating we have

$$\chi_\infty = \frac{1}{e^\gamma (1 + 1/\chi_f) - 1} \quad (3.23)$$

where $\chi_\infty = \chi(T = 0)$, $\chi_f = \chi(T = \Lambda)$ and

$$\gamma \equiv \frac{2fN_f \langle \sigma v \rangle_0}{3H_1} \sqrt{\frac{\Lambda}{M}} \sim \frac{M_P N_f}{\Lambda^4} \sqrt{\frac{\Lambda}{M}} \quad (3.24)$$

This is typically huge because of it is proportional to M_P/Λ . N_f/Λ^3 depends on initial conditions, but is typically $\ll 1$ (for a review, see [97] and references therein). In this case we have $\chi_\infty \sim e^{-\gamma}$ so that few excited states are left after the second freezeout. Even for the extreme values of $N_f/\Lambda^3 \sim 10^{-15}$, $\Lambda = 1$ MeV, $M = 1$ TeV we have $\gamma \sim 10^3$, so the relic abundance of excited states is indeed quite small.

3.5 Annihilation for excited states

If two particles which can annihilate form a bound state with $J > 0$ their annihilation rate will be suppressed by an additional α^{2l} compared to the S -state. This phenomenon was well studied during the formative years of quantum field theory, but recently is quite obscure [81, 82]. (There is a little discussion of the matter in standard texts on quantum field theory [2, 3]. For useful reviews on bound-state physics, see [83, 84].) The reason for this is obvious, in the most often studied case, positronium, radiative decays dominate so that typically annihilation will not occur from the P -state. However, if a radiative decay is impossible, annihilation from $J > 0$ again becomes relevant.

The picture usually given is that the annihilation rate is proportional to the probability to find the constituents in the same place $|\psi(0)|^2$. This is not only misleading but erroneous. One way to see that this picture does not make sense is to note that both particles in the bound state are described by non-localized wavefunctions, and in the case of positronium these are identical so that their overlap is unity. The real origin of the dependence on $|\psi(0)|^2$ is from the momentum space overlap of the unbound final state with the initial bound state. We

can construct a bound state

$$|B\rangle = \sqrt{2M} \int \frac{d^3k}{(2\pi)^3} \tilde{\psi}_i(\vec{k}) \Sigma_{ab}^i(J) \frac{1}{2m} |\phi_a^+(\vec{k}); \phi_b^-(-\vec{k})\rangle \quad (3.25)$$

where ϕ^\pm are particles (spin unspecified) and $M = 2m - E_b$ where E_b is the binding energy. $\Sigma_{ab}^i(J)$ is a matrix which connects the wavefunctions to the Fock state with the appropriate spin and depends on the total angular momentum J . The annihilation amplitude is therefore

$$\mathcal{M}(B \rightarrow f) = \frac{\sqrt{2M}}{2m} \int \frac{d^3k}{(2\pi)^3} \tilde{\psi}_i(\vec{k}) \Sigma_{ab}^i \mathcal{M}(\phi_a^+ \phi_b^- \rightarrow f) \quad (3.26)$$

where $\mathcal{M}(\phi_a^+ \phi_b^- \rightarrow f)$ is an ordinary free-scattering amplitude. From this we see the origin of the α^{2l} suppression. Since the momenta in the bound state are $\sim \alpha m$, from the momentum dependence in $\mathcal{M}(\phi_a^+ \phi_b^- \rightarrow f)$ one has, to lowest order

$$\int \frac{d^3k}{(2\pi)^3} k^i \tilde{\psi}(\vec{k}) = i \partial_i \psi(\vec{x}) \Big|_{\vec{x}=0} \rightarrow \alpha \quad (3.27)$$

It takes l derivatives of a wavefunction of angular momentum l to obtain a function which does not vanish at the origin for central potentials, so the leading term contains a α^{2l} suppression. This effect may be greater depending on the structure of $\mathcal{M}(\phi_a^+ \phi_b^- \rightarrow f)$, for instance, if it only depends on k^2 . Note that for a strongly coupled theory, inside the confining potential we expect effectively $\alpha \sim 10^{-1}$ or larger [85, 86].

We see that the suppression of the annihilation rate is not exponential, so it is certainly not the many orders of magnitude needed to make moderately high l bound states viable as meta-stable dark matter. In scenarios where hidden sector bound states decay shortly before nucleosynthesis however, this may be an important consideration, as decays of high l states are still delayed by several orders of magnitude depending on the parameters.

3.6 Summary on Orbitally Excited Dark Matter

We have seen that orbitally excited DM is unlikely to play a significant roll in cosmology, regardless of the details of the specific model. If DM bound states are composed of constituents which can annihilate, even for high l this process will occur on time-scales only several orders of magnitude longer than $1/M$, which is typically nowhere near cosmic timescales. For very high l we expect DM of this kind to be unstable against decay to glueballs anyway. If a substantial portion of stable bound-state DM particles emerge from a phase transition in excited states, we expect these to de-excite through collisions, even when they are stable. In cases where there is more than one flavor, it is energetically favorable for these collisions to result in particle-anti-particle bound states which can annihilate [100]. Though this process freezes out, the remaining relative abundance of excited states is expected to be exponentially suppressed.

APPENDIX A
CPV RELATED TOPICS

A.1 Some Explicit Expressions for Kaon Mixing

In this appendix we collect more general expressions relevant for extracting γ from $B^\pm \rightarrow DK^\pm$, taking into account kaon oscillations, that we omit in the main text. In the main text we usually kept the γ dependence explicit, while here we keep the time dependence explicit. Consider a D meson state which results from the decay of the B^- and which is a superposition of D^0 and \bar{D}^0 depending on $A_B, r_B, \delta_B, \gamma$. We denote that state D_B . It is useful to write quantities in terms of D_B decay amplitudes. We define

$$c_{K^0} \equiv A(D_B \rightarrow K^0 \pi^+ \pi^-), \quad c_{\bar{K}^0} \equiv A(D_B \rightarrow \bar{K}^0 \pi^+ \pi^-). \quad (\text{A.1})$$

We also define $c_{L,S}$ to be c_{K^0} with the K^0 replaced by $K_{L,S}$. These amplitudes are simply related

$$c_S \equiv \frac{1}{2pq} (qc_{K^0} - pc_{\bar{K}^0}), \quad c_L \equiv \frac{1}{2pq} (qc_{K^0} + pc_{\bar{K}^0}), \quad (\text{A.2})$$

and can be expressed in terms of γ

$$c_{K^0} = A_B (A_D r_D e^{i\delta_D} + \bar{A}_D r_B e^{i(\delta_B - \gamma)}), \quad (\text{A.3})$$

$$c_{\bar{K}^0} = A_B (A_D + \bar{A}_D r_B \bar{r}_D e^{i(\delta_B + \bar{\delta}_D - \gamma)}). \quad (\text{A.4})$$

These can be written for the B^+ by $\gamma \rightarrow -\gamma$ and $(A_D, r_D, \delta_D) \leftrightarrow (\bar{A}_D, \bar{r}_D, \bar{\delta}_D)$. The latter is equivalent to changing the sign of ϵ in the overall decay width. The kaon time dependent overall width of the $B \rightarrow DK$ followed by $D \rightarrow K\pi\pi$ and then $K \rightarrow \pi\pi$

$$\frac{d^2\Gamma}{ds^2}(B^- \rightarrow f^-) = |A_{\pi\pi}|^2 (|c_S|^2 e^{-\Gamma_S t} + |\epsilon c_L|^2 e^{-\Gamma_L t} + 2e^{-\Gamma t} \text{Re}(\epsilon^* c_L^* c_S e^{ix\Gamma t})), \quad (\text{A.5})$$

where f^- is defined in (1.30). When expanding $|c_S|^2$ and $c_L^* c_S$ there are a number of expressions which occur frequently, we define

$$\begin{aligned}
F_D &\equiv |A_D|^2 (1 + r_D^2 - 2r_D \cos(\delta_D)), \\
F'_D &\equiv \text{Re}(A_D^* \bar{A}_D) - 2r_D \text{Re}(A_D^* \bar{A}_D e^{-i\delta_D}) - r_D \bar{r}_D \text{Re}(A_D^* \bar{A}_D e^{i(\bar{\delta}_D - \delta_D)}), \\
\kappa_D &\equiv |A_D|^2 (1 - r_D^2 - 2r_D \sin(\delta_D)), \\
\kappa'_D &\equiv |A_D|^2 (1 - r_D^2 + 2r_D \sin(\delta_D)),
\end{aligned} \tag{A.6}$$

with barred quantities can be obtained by $(A_D, r_D, \delta_D) \rightarrow (\bar{A}_D, \bar{r}_D, \bar{\delta}_D)$. Neglecting terms of order $r_B |\epsilon|$ we get, for example,

$$|c_S|^2 = \frac{|A_B|^2}{2} \left[F_D + r_B^2 \bar{F}_D + 2\kappa_D \text{Re}(\epsilon) - 2r_B F'_D \cos(\delta_B - \gamma) \right], \tag{A.7}$$

$$\epsilon^* c_L^* c_S = -\frac{|A_B A_D|^2}{2} \epsilon^* (1 - r_D^2 - 2ir_D \sin(\delta_D)). \tag{A.8}$$

When integrating over all of time, these combine giving expressions which include κ'_D , so that κ'_D/F'_D appears in the expression for $\Delta\gamma$.

Integrals over time involve a detection efficiency function $F(t)$ which must be determined for a particular experiment. As an illustrative example, consider $F(t) = 1$ for $t_1 < t < t_2$ and $F(t) = 0$ otherwise. The following integrals involving an arbitrary complex number z may also be useful

$$\Gamma_S \int_{t_1}^{t_2} dt \text{Re}(z^* e^{\Gamma t(ix-1)}) = (x\text{Re}(z) - \text{Im}(z))Q_c(t_1, t_2) + (\text{Im}(z) - x\text{Re}(z))Q_s(t_1, t_2), \tag{A.9}$$

$$\Gamma_S \int_{t_1}^{t_2} dt \text{Im}(z^* e^{\Gamma t(ix-1)}) = (x\text{Re}(z) - \text{Im}(z))Q_c(t_1, t_2) + (\text{Re}(z) + x\text{Im}(z))Q_s(t_1, t_2), \tag{A.10}$$

where

$$Q_c(t_1, t_2) = -\frac{1-y}{1+x^2} \left[e^{-\Gamma t_2} \cos(x\Gamma t_2) - e^{-\Gamma t_1} \cos(x\Gamma t_1) \right], \tag{A.11}$$

$$Q_s(t_1, t_2) = -\frac{1-y}{1+x^2} \left[e^{-\Gamma t_2} \sin(x\Gamma t_2) - e^{-\Gamma t_1} \sin(x\Gamma t_1) \right], \tag{A.12}$$

where we have used $\Gamma_S = (1 - y)\Gamma$. While we have not used any approximation involving the variables x, y , it greatly simplifies things to use $x \approx -y \approx 1$, which we use in the main body of the chapter when estimating $\Delta\gamma$. When integrating over all time we have $Q_c(0, \infty) = (1 - y)/(1 + x^2) \approx 1$ and $Q_s(0, \infty) = 0$.

It is also useful to have an expansion of $\mathcal{A}^*\mathcal{A}$. Note that

$$\text{Re}(\mathcal{A}^*\mathcal{A}) = \text{Re}(A_S^*\bar{A}_S)e^{-\Gamma_S t} + |\epsilon|^2 \text{Re}(A_L^*\bar{A}_L)e^{-\Gamma_L t} + \text{Re}\left[\epsilon^*(A_S\bar{A}_L^* + A_L^*\bar{A}_S)e^{\Gamma t(ix-1)}\right], \quad (\text{A.13})$$

$$\text{Im}(\mathcal{A}^*\mathcal{A}) = \text{Im}(A_S^*\bar{A}_S)e^{-\Gamma_S t} + |\epsilon|^2 \text{Im}(A_L^*\bar{A}_L)e^{-\Gamma_L t} + \text{Im}\left[\epsilon^*(-A_S\bar{A}_L^* + A_L^*\bar{A}_S)e^{\Gamma t(ix-1)}\right]. \quad (\text{A.14})$$

Therefore, in terms of $\theta_D(s_{12}, s_{13}) \equiv \arg(A_D^*\bar{A}_D)$ to order $|\epsilon|$ we obtain

$$A_S^*\bar{A}_S = \frac{|A_D^*\bar{A}_D|}{2} e^{i\theta_D} \left[1 + (1 - 2\text{Re}(\epsilon))r_D\bar{r}_D e^{i(\bar{\delta}_D - \delta_D)} - r_D e^{-i\delta_D} - \bar{r}_D e^{i\bar{\delta}_D} \right. \quad (\text{A.15})$$

$$\left. - 2ir_D e^{-i\delta_D} \text{Im}(\epsilon) + 2i\bar{r}_D e^{i\bar{\delta}_D} \text{Im}(\epsilon) \right], \quad (\text{A.16})$$

$$\epsilon^* A_S \bar{A}_L^* = \epsilon^* \frac{|A_D^*\bar{A}_D|}{2} e^{-i\theta_D} \left(r_D e^{i\delta_D} - 1 - \bar{r}_D e^{-i\bar{\delta}_D} + r_D \bar{r}_D e^{i(\delta_D - \bar{\delta}_D)} \right). \quad (\text{A.17})$$

A.2 Other Small Weak Phases

There are two other sources of CP violation which we have not taken into account, but which may become important at the $r_B|\epsilon|$ level. Neither of these present any significant complication to the methods discussed in the body of the letter where they are largely ignored, and they are simply accounted for, at least to the extent to which they can be accurately measured in other experiments.

A.2.1 In $D \rightarrow K\pi^+\pi^-$

There is a small amount of CP violation involved in the decay of the D . This plays much the same role as the CP violation in the kaon mixing and decay, both are like CP violation in the D decay for the intents and purposes of the Dalitz analysis. Regardless of how small the CP violation is in the D decay itself, this is already taken into account when neglecting $r_B|\epsilon|$ terms when we allow for $T_i^+ \neq T_i^-$. This CP violation makes its appearance in the variables δ_D and $\bar{\delta}_D$. This can be taken into account for all terms (including $r_B|\epsilon|$ terms) by allowing for $\delta_D(s_{12}, s_{13}) \neq \bar{\delta}_D(s_{13}, s_{12})$. In fact

$$\frac{\delta_D(s_{12}, s_{13}) - \bar{\delta}_D(s_{13}, s_{12})}{2} = \arg\left(\frac{V_{us}V_{cd}^*}{V_{ud}V_{cs}^*}\right). \quad (\text{A.18})$$

Note that $V_{us}V_{cd}^*/V_{ud}V_{cs}^* \sim \lambda^2$ with a non-zero phase coming in at $O(\lambda^6)$. This is of course extremely small, but it may be compensated for by kinematic effects in some regions of phase space (i.e. where r_D is not small). In that case the phase can be thought of as a λ^4 correction, which may be competitive with $O(|\epsilon|)$ effects. As noted however, this is most important in the T_i^\pm terms where it is already taken into account, otherwise it is suppressed by r_B .

A.2.2 In $B^\pm \rightarrow DK^\pm$

The weak angle involved in the decay $B^\pm \rightarrow DK^\pm$ is not precisely γ but receives some small corrections from other CKM elements. The ratio of CKM matrix elements involved in the decay is $V_{cs}V_{ub}^*/V_{us}V_{cb}^*$. Relating this to γ involves

$$\frac{V_{cd}V_{cs}}{V_{ud}V_{us}} = -1 + A^2\lambda^4 - A^2\lambda^4(\rho + i\eta) + O(\lambda^6). \quad (\text{A.19})$$

From this we see that corrections to the phase $e^{-i\gamma}$ come in at order $\lambda^4 \sim 10^{-3}$. This is still unimportant at the $|\epsilon|/r_B$ level but is competitive with $O(|\epsilon|)$ corrections. In all previous sections where we have written γ , we in fact mean $\gamma + \phi_B$ where

$$\phi_B \equiv \arg\left(\frac{V_{cd}V_{cs}}{V_{ud}V_{us}}\right). \quad (\text{A.20})$$

This can be considered a fundamental limitation on $B^\pm \rightarrow DK^\pm$ methods, although it can be overcome to whatever accuracy ϕ_B can be measured by other means.

A.3 Unbinned Analysis

It is possible to perform an unbinned analysis for extracting γ from $B^\pm \rightarrow DK^\pm$, instead fitting directly the probability density function

$$f(s_{12}, s_{13}|\phi) = |A^2(B^+ \rightarrow (K_S^0\pi^+\pi^-)_D K^+)|^2 \quad (\text{A.21})$$

to the observed data points. Such an approach would clearly require an explicit model for the D decay amplitude. Though the fits to resonance models are impressive [8, 32] uncertainty in the resonance model fit parameters is much greater than the minimum attainable statistical uncertainty in γ from binned methods [7].

It is instructional however to compare the unbinned analysis to the binned one, and it may be possible that advances in resonance models will one day make an unbinned approach feasible (though this subject would need to be investigated further).

For simplicity, let's consider a fixed number of events N . In this case the log

likelihood function for the unbinned fit is given by

$$-\log(L(\phi)) = -\sum_{i=1}^N \log(f(\vec{s}_i|\phi)) \quad (\text{A.22})$$

where $\vec{s}_i = (s_{12}^i, s_{13}^i)$ is the location in phase space of the i th event. The statistical uncertainty in ϕ , as before, is given by

$$\sigma_\phi^2 = -\left(\frac{\partial^2 \log(L)}{\partial \phi^2}\right)^{-1} \quad (\text{A.23})$$

and again for simplicity we treat it as the only parameter being fitted for. We can express this more explicitly as

$$\sigma_\phi^{-2} = \sum_{i=1}^N \left(-\frac{1}{f_i} \frac{\partial^2 f_i}{\partial \phi^2} + \frac{1}{f_i^2} \left(\frac{\partial f_i}{\partial \phi} \right)^2 \right) \quad (\text{A.24})$$

where $f_i = f(\vec{s}_i|\phi)$.

In reality of course, things are much more complicated, because many other variables need to be fitted as well. However, if one were to consider the case where, for example, all parameters in a model for $f(\vec{s}|\phi)$ were already fitted in other experiments, then things really do become this simple, with the exception of systematic uncertainties.

Far more data should be available for most of the parameters in $f(\vec{s}|\phi)$ than for ϕ , since (in theory) those parameters can be measured in any experiment where there are D decays. The only exception (other than ϕ of course) is the color and Cabbibo suppression parameter r_B .

A.4 Variational Calculus Approach for Improving Binning

A generalized method for performing a measurement in such a way that it minimizes statistical uncertainty have been suggested [40] and implemented suc-

cessfully [38]. Unfortunately it is not so clear how to generalize this method to a binned likelihood fit, and our case is made quite a bit more complicated by the form of (1.76), as opposed to, say, the uncertainty in the measurement of a single independent variable. Still, this suggests a method with which we might proceed.

We can treat our bins as functions such that

$$F_i = \int d^2\xi \kappa_i(\vec{\xi}) f(\vec{\xi}|\phi) \quad (\text{A.25})$$

In the cases we have been considering the κ_i are just complicated θ functions. To make sense as bins these should cover the space, such that

$$\sum_{i=1}^N \int d^2\xi \kappa_i(\vec{\xi}) g(\vec{\xi}) = \int d^2\xi g(\vec{\xi}) \quad (\text{A.26})$$

where g is any function.

Using variational calculus to extremize (1.76) we have the following

$$\sum_{i=1}^N \left[\frac{2}{F_i} \frac{\partial F_i}{\partial \phi} \int d^2s \frac{\partial f}{\partial \phi} - \frac{1}{F_i^2} \left(\frac{\partial F_i}{\partial \phi} \right)^2 \int d^2s f \right] + N \int d^2s g = 0 \quad (\text{A.27})$$

Here g is treated as a Lagrange multiplier such that (A.26) holds true. Using the constraint we note

$$\int d^2s f = \sum_{i=1}^N \int d^2s \kappa_i f = \sum_{j=1}^N F_j \quad (\text{A.28})$$

$$\int d^2s \frac{\partial f}{\partial \phi} = \sum_{i=1}^N \int d^2s \kappa_i \frac{\partial f}{\partial \phi} = \sum_{j=1}^N \frac{\partial F_j}{\partial \phi} \quad (\text{A.29})$$

so that

$$\left(\sum_{j=1}^N \frac{\partial F_j}{\partial \phi} \right) \left(\sum_{i=1}^N \frac{2}{F_i} \frac{\partial F_i}{\partial \phi} \right) - \left(\sum_{j=1}^N F_j \right) \left(\sum_{i=1}^N \frac{1}{F_i^2} \left(\frac{\partial F_i}{\partial \phi} \right)^2 \right) + N \int d^2s g = 0 \quad (\text{A.30})$$

This can be converted into an integro-differential equation for the functions κ_i . Unfortunately, converting this into a differential form will result in the accumulation of non-vanishing boundary terms. To be useful (A.30) should be written in terms of κ_i , but the result was too complicated to seem useful.

A.5 BinOptimize Code

We developed a C++ program for implementing and testing the various binning methods. This program included objects for calculating amplitudes as well as re-binning and optimizing the function contour intervals so as to obtain more efficient binning. The program will be made available if requested for anyone interested. Below is an overview of the includes

- `Particle.h` Contains pre-compiler constants as well as an object for implementing particles in a decay.
- `Resonance.h` Contains an object for calculating resonance shapes.
- `Decay.h` Contains the `Decay` object for calculating kinematic limits and the Dalitz distribution of a decay.
- `Amplitudes.h` Contains objects for calculating amplitudes of decays.
- `EventGen.h` Contains objects for implementing a Monte Carlo simulation of a decay.
- `Overbin.h` Contains objects for binning amplitudes or Monte Carlo generated data in the various ways discussed in the chapter.
- `Optimizers.h` Contains objects used for optimizing binning.

APPENDIX B
ORBITALLY EXCITED DM APPENDIX

B.1 Derivation of Boltzmann Equations

For a review on DM and the application of Boltzmann equations to the subject see [97] and references therein. In a Friedman-Robertson-Walker manifold, the condition that a number density is conserved is simply

$$\frac{d}{dt}(n_i a^3) = 0 \quad (\text{B.1})$$

so that we can postulate the Boltzmann equation

$$\frac{1}{a^3} \frac{d}{dt}(n_i a^3) = - \sum_{k,l} \alpha_{kl} n_k n_l \quad (\text{B.2})$$

where the α 's are simply related to thermal average cross-sections. Suppose we have a system with $s + 1$ possible states. It is useful to define

$$X_i \equiv \frac{n_i}{N}, \quad N \equiv \sum_{j=0}^s n_j \quad (\text{B.3})$$

Differentiating we have

$$\frac{dX}{dt} = \frac{1}{Na^3} \frac{d}{dt}(n_i a^3) - \frac{n_i a^3}{N^2 a^6} \frac{d}{dt}(Na^3) \quad (\text{B.4})$$

We postulate that this can be written

$$\frac{dX}{dt} = -\frac{1}{N} \sum_{k,l} \alpha_{kl} n_k n_l = -N \sum_{k,l} \alpha_{kl} X_k X_l \quad (\text{B.5})$$

Using $H \equiv (da/dt)/a$ and $d \log(a) = -d \log(T)$ this can be written

$$\frac{d \log(X_i)}{d \log(T)} = \frac{N}{H} \left(\frac{1}{X_i} \sum_{k,l} \alpha_{kl} X_k X_l \right) \quad (\text{B.6})$$

One can then use the scaling properties of $N = T^3 N_f / T_f^3$ and H to write this

$$\frac{d \log(X_i)}{d \log(T)} = T \frac{\Lambda^2 (N_f / T_f^3)}{H_1} \left(\frac{1}{X_i} \sum_{k,l} \alpha_{kl} X_k X_l \right) \quad (\text{B.7})$$

The above is only valid if hidden sector particles do not decay into something else, i.e. if $d(Na^3)/dt = 0$. If this is not the case, writing the Boltzmann equation in terms of the fractional abundance X_i is not useful, one should instead use (B.2). Defining $Y_i \equiv n_i/T^3$, this can be written in the more conventional way

$$\frac{dY}{d \log(T)} = \frac{T^3}{H} \sum_{k,l} \alpha_{kl} Y_k Y_l \quad (\text{B.8})$$

Similar forms can be found in any standard text on thermal cosmology.

The α coefficients are simply related to thermal average cross-sections and decay rates. One should only sum over α 's which involve the particle species which appears on the left side of the equation. For example, if we suppose we can have the reaction $AB \leftrightarrow CD$ and A can also decay, one should write the right side of (B.2)

$$-\langle \sigma v \rangle n_A n_B + \langle \sigma v \rangle n_C n_D - \Gamma n_A \quad (\text{B.9})$$

so that $\alpha_{AB} = \langle \sigma v \rangle$, $\alpha_{CD} = -\langle \sigma v \rangle$ and $\alpha_{A0} = \Gamma$ are the only non-vanishing coefficients. Again, this sort of thing can be found in standard texts.

To estimate the relative abundance in a two-level system, it is simplest to write the Boltzmann equation in terms of $\chi \equiv n_1/n_0$. This allows us to eliminate one of the equations. Using (B.2) and the fact that with no decays we have $d(n_0 a^3)/dt = -d(n_1 a^3)/dt$ we have

$$\frac{d\chi}{dy} = \frac{N_f}{H_1} (\alpha_{11} \chi^2 + \alpha_{10} \chi) \quad (\text{B.10})$$

where $y := T/\Lambda$ and $N_f = (n_0 + n_1)|_{T=\Lambda}$.

B.2 Thermal Average Cross-section

We review some basic facts about the thermal average cross-section $\langle\sigma v\rangle$ so it can be computed in a more general case than we considered in the text. One defines

$$\langle\sigma_{ab}v\rangle = \frac{g_a g_b}{n_a^{(eq)} n_b^{(eq)}} \int \frac{d^3 p_a}{(2\pi)^3} \int \frac{d^3 p_b}{(2\pi)^3} f_a^{(eq)} f_b^{(eq)} \sigma_{ab}(p_a, p_b) v \quad (\text{B.11})$$

where g_a is the degeneracy of species a and $f_a^{(eq)}$ is its statistical distribution (i.e. Fermi or Bose-Einstein). v is the relative velocity $|p_a/E_a - p_b/E_b|$. $n_a^{(eq)} = \int \frac{d^3 p}{(2\pi)^3} f_a^{(eq)}$ is the equilibrium number density. In the non-relativistic case in which we are interested it is given by

$$n_a^{(eq)} = g_a \left(\frac{m_a T}{2\pi} \right)^{3/2} e^{-m_a/T} \quad (\text{B.12})$$

In the main text of this chapter we alluded to thermal average cross-section for particles of distinct masses with a constant scattering cross-section, but did not write it explicitly. It can be written in terms of error functions

$$\langle\sigma_{ab}v\rangle = \frac{g_a g_b}{n_a^{(eq)} n_b^{(eq)}} \frac{m_a^3 m_b^3}{3 \cdot 2^5 (2\pi)^4} \sigma_{tot} e^{-(m_a+m_b)/T} I(m_a, m_b, T) \quad (\text{B.13})$$

where

$$\begin{aligned} I(m_a, m_b, T) &= \int_0^\infty dx \int_0^\infty dy e^{-(m_a x^2 + m_b y^2)/2T} xy(x+y)^3 \\ &\quad - \int_y^\infty dx \int_0^\infty dy e^{-(m_a x^2 + m_b y^2)/2T} xy(x-y)^3 \\ &\quad - \int_0^\infty dx \int_x^\infty dy e^{-(m_a x^2 + m_b y^2)/2T} xy(y-x)^3 \end{aligned} \quad (\text{B.14})$$

Using dimensional analysis (and noting the T dependence of $1/(n_a^{(eq)} n_b^{(eq)})$) we expect that this complicated function will have similar T dependence to the case of identical particles, but clearly the exact function is quite complicated.

B.3 Model for Semi-Elastic De-excitation Interactions

Our starting point for estimating a cross-section is a partial wave expansion of the scattering amplitude for particles of arbitrary spin and helicity [91, 92]

$$f_{\lambda\lambda'}(\theta) = \sum_{j=\lambda_{max}}^{\infty} (2j+1) f_{\lambda\lambda'}^j d_{\lambda\lambda'}^j(\theta) \quad (\text{B.15})$$

where $\lambda = \lambda_1 - \lambda_2$ is the difference in initial state helicities, and $\lambda' = \lambda'_1 - \lambda'_2$ is the difference in final state helicities. The functions $d_{\lambda\lambda'}^j(\theta)$ are the Wigner rotation matrices, Normally one would insert δ functions into the appropriate definitions to prevent the spin of particles from changing in an interaction, but without doing so the above is valid for arbitrary spins of initial and final states [92]. Note that the sum, which would begin at $j = 0$ in the scalar case, is now cut off at λ_{max} . This aligns with our intuitive notion that internal angular momentum which is lost must appear as orbital angular momentum in the final state, so that $J < \lambda_{max}$ terms do not contribute.

Now, to choose partial scattering amplitudes $f_{\lambda\lambda'}^j$ we borrow intuition from the scalar case. We assume a hard-sphere interaction (which is sometimes used to treat nucleon-nucleon scattering [93], which is not so dissimilar from our case) for spheres of radius $1/\Lambda$. The $j = 0$ term for this famously results in a geometric cross-section, $\sigma_{tot} \propto 1/\Lambda^2$ (see also [94]). The partial amplitudes for higher j are strongly suppressed by additional powers of (k/Λ) where k is the center of mass momentum, as well as $[(2j-1)!!]^{-2}$ [95]. Scattering amplitudes typically do not change by many orders of magnitude when considering particles of different spin (unless symmetry forbids certain terms) so we will assume the expansion is of the same order of magnitude in our case order by order. The critical difference is that now, our expansion is cut off at λ_{max} . Treating the

$j > 0$ terms as higher order, this indicates that to leading order only collisions between particles with anti-aligned spins can contribute. Using the result from the scalar case we take the total cross-section for these collisions to be, simply

$$\sigma_{tot} = \frac{4\pi}{\Lambda^2} \quad (\text{B.16})$$

B.4 Reheating Through Collisional De-excitation, Details

The condition that must be satisfied for this sort of reheating not to occur is

$$\Lambda N^2 \langle \sigma v \rangle \ll \left| \frac{\partial \rho_{DM}}{\partial t} \right|_{\text{expansion}} \quad (\text{B.17})$$

That is, the amount of energy injected by de-excitation (roughly Λ per interaction) must be much less than the energy the DM gas loses as it cools through expansion. This condition assumes that a sizable portion of the DM particles are in excited states, which we were already assuming for early times. In the non-relativistic regime

$$\left| \frac{\partial \rho}{\partial T} \right| \sim M \left| \frac{\partial N}{\partial T} \right| = M \left| \frac{dT}{dt} \right| \left(3 \frac{N}{T} \right) \quad (\text{B.18})$$

where we have used that, in a radiation dominated universe $T \sim M_P (M_P/t)^{1/2}$ so that $dT/dt \sim -T^3/M_P$ which gives

$$\left| \frac{\partial \rho}{\partial t} \right|_{\text{expansion}} \sim \frac{MNT^2}{M_P} \quad (\text{B.19})$$

This gives

$$\left(\frac{T}{M} \right)^{3/2} \ll \frac{M\Lambda}{H_0^2 M_P^3 / T_0^3} \quad (\text{B.20})$$

or

$$\left(\frac{T}{M} \right)^{3/2} \ll \left(\frac{M\Lambda}{10^9 \text{ GeV}^2} \right) \quad (\text{B.21})$$

as the condition which must be satisfied for reheating to end. Note that we have again assumed a constant cross-section $\sigma \sim 1/\Lambda^2$. In the region of parameter space where $T_r = M(M\Lambda/10^9 \text{ GeV}^2)^{2/3} > \Lambda$, the reheating process never takes place since this condition is always satisfied after the phase transition.

BIBLIOGRAPHY

- [1] G. C. Branco, L. Lavoura and J. P. Silva, “CP violation”, Clarendon Press (1999).
- [2] C. Itzykson, J. B. Zuber, *Quantum Field Theory*, Dover, 1980
- [3] M. E. Peskin, D. V. Schroeder, *An Introduction to Quantum Field Theory*, Westview, 1995
- [4] H. K. Dreiner, H. E. Haber and S. P. Martin, Phys. Rept. **494**, 1 (2010) [arXiv:0812.1594 [hep-ph]].
- [5] M. Gronau and D. Wyler, Phys. Lett. B **265**, 172 (1991).
- [6] D. Atwood, I. Dunietz and A. Soni, Phys. Rev. D **63**, 036005 (2001) [hep-ph/0008090].
- [7] A. Giri, Y. Grossman, A. Soffer and J. Zupan, Phys. Rev. D **68**, 054018 (2003) [hep-ph/0303187].
- [8] A. Poluektov *et al.* [Belle Collaboration], Phys. Rev. D **70**, 072003 (2004) [hep-ex/0406067].
- [9] M. Gronau and D. London, Phys. Lett. B **253**, 483 (1991).
- [10] B. Kayser and D. London, Phys. Rev. D **61**, 116013 (2000) [hep-ph/9909561].
- [11] Y. I. Azimov and A.A. Iogansen, Yad. Fiz. **33**, 388 (1981) [Sov. J. Nucl. Phys. **33**, 205 (1981)].
- [12] Y. I. Azimov, Eur. Phys. J. A **4**, 21 (1999) [hep-ph/9808386].
- [13] H. J. Lipkin, Z. -z. Xing, Phys. Lett. **B450**, 405-411 (1999). [hep-ph/9901329].
- [14] I. I. Bigi, A. I. Sanda, Phys. Lett. **B625**, 47-52 (2005). [hep-ph/0506037].
- [15] G. Calderon, D. Delepine, G. L. Castro, Phys. Rev. **D75**, 076001 (2007). [hep-ph/0702282 [HEP-PH]].

- [16] Y. Grossman and Y. Nir, JHEP **1204**, 002 (2012) [arXiv:1110.3790 [hep-ph]].
- [17] Y. Grossman, A. Soffer and J. Zupan, Phys. Rev. D **72**, 031501 (2005) [hep-ph/0505270].
- [18] J. P. Silva and A. Soffer, Phys. Rev. D **61**, 112001 (2000) [hep-ph/9912242].
- [19] A. Amorim, M. G. Santos and J. P. Silva, Phys. Rev. D **59**, 056001 (1999) [hep-ph/9807364].
- [20] M. Rama, arXiv:1307.4384 [hep-ex].
- [21] M. Gronau, Y. Grossman and J. L. Rosner, Phys. Lett. B **508**, 37 (2001) [hep-ph/0103110].
- [22] A. Soffer, hep-ex/9801018.
- [23] A. Soffer, Phys. Rev. D **60**, 054032 (1999) [hep-ph/9902313].
- [24] D. Atwood and A. Soni, Phys. Rev. D **68**, 033003 (2003) [hep-ph/0304085].
- [25] E. M. Aitala *et al.* [E791 Collaboration], Phys. Rev. Lett. **86**, 770 (2001).
- [26] P. del Amo Sanchez *et al.* [BaBar Collaboration], Phys. Rev. Lett. **105**, 121801 (2010) [arXiv:1005.1096 [hep-ex]].
- [27] A. Poluektov *et al.* [Belle Collaboration], Phys. Rev. D **81**, 112002 (2010) [arXiv:1003.3360 [hep-ex]].
- [28] H. Muramatsu *et al.* [CLEO Collaboration], Phys. Rev. Lett. **89**, 251802 (2002) [Erratum-ibid. **90**, 059901 (2003)] [hep-ex/0207067].
- [29] J. Brod and J. Zupan, arXiv:1308.5663 [hep-ph].
- [30] M. Schlupp, arXiv:1307.7018 [hep-ex].
- [31] T. Aushev, W. Bartel, A. Bondar, J. Brodzicka, T. E. Browder, P. Chang, Y. Chao and K. F. Chen *et al.*, arXiv:1002.5012 [hep-ex].
- [32] S. Kopp *et al.* [CLEO Collaboration], Phys. Rev. D **63**, 092001 (2001) [hep-ex/0011065].

- [33] Belle II Collaboration, [arxiv:1011.0352]
- [34] A. Bondar and A. Poluektov, Eur. Phys. J. C **55**, 51 (2008) [arXiv:0801.0840 [hep-ex]].
- [35] J. Libby *et al.* [CLEO Collaboration], Phys. Rev. D **82**, 112006 (2010) [arXiv:1010.2817 [hep-ex]].
- [36] Y. Grossman and M. Savastio, JHEP **1403**, 008 (2014) [arXiv:1311.3575 [hep-ph]].
- [37] R. Aaij *et al.* [LHCb Collaboration], arXiv:1408.2748 [hep-ex].
- [38] D. Atwood, I. Dunietz and A. Soni, Phys. Rev. Lett. **78**, 3257 (1997) [hep-ph/9612433].
- [39] I. Fister Jr., X. S. Yang, D. Fister, I. Fister, [arXiv:1408.5343]
- [40] D. Atwood and A. Soni, Phys. Rev. D **45**, 2405
- [41] J. M. Cline, hep-ph/0609145.
- [42] D. E. Morrissey and M. J. Ramsey-Musolf, New J. Phys. **14**, 125003 (2012) [arXiv:1206.2942 [hep-ph]].
- [43] A. Katz and M. Perelstein, JHEP **1407**, 108 (2014) [arXiv:1401.1827 [hep-ph]].
- [44] S. Davidson, E. Nardi and Y. Nir, Phys. Rept. **466**, 105 (2008) [arXiv:0802.2962 [hep-ph]].
- [45] W. Buchmuller, P. Di Bari and M. Plumacher, Annals Phys. **315**, 305 (2005) [hep-ph/0401240].
- [46] M. C. Chen, hep-ph/0703087 [HEP-PH].
- [47] R. Barbier, C. Berat, M. Besancon, M. Chemtob, A. Deandrea, E. Dudas, P. Fayet and S. Lavignac *et al.*, Phys. Rept. **420**, 1 (2005) [hep-ph/0406039].
- [48] C. Smith, arXiv:0809.3152 [hep-ph].

- [49] E. Nikolidakis and C. Smith, Phys. Rev. D **77**, 015021 (2008) [arXiv:0710.3129 [hep-ph]].
- [50] C. Csaki, Y. Grossman and B. Heidenreich, Phys. Rev. D **85**, 095009 (2012) [arXiv:1111.1239 [hep-ph]].
- [51] G. D'Ambrosio, G. F. Giudice, G. Isidori and A. Strumia, Nucl. Phys. B **645**, 155 (2002) [hep-ph/0207036].
- [52] E. A. Baltz and P. Gondolo, Phys. Rev. D **57**, 7601 (1998) [hep-ph/9704411].
- [53] M. Endo, K. Hamaguchi and S. Iwamoto, JCAP **1002**, 032 (2010) [arXiv:0912.0585 [hep-ph]].
- [54] A. Ibarra, In *Karlsruhe 2007, SUSY 2007* 934-937 [arXiv:0710.2287 [hep-ph]].
- [55] B. Batell, T. Lin and L. -T. Wang, JHEP **1401**, 075 (2014) [arXiv:1309.4462 [hep-ph]].
- [56] S. P. Martin, In *Kane, G.L. (ed.): Perspectives on supersymmetry II* 1-153 [hep-ph/9709356].
- [57] V. Khachatryan *et al.* [CMS Collaboration], JHEP **1103**, 024 (2011) [arXiv:1101.1645 [hep-ex]].
- [58] G. Aad *et al.* [ATLAS Collaboration], Phys. Lett. B **703**, 428 (2011) [arXiv:1106.4495 [hep-ex]].
- [59] J. M. Cline and K. Kainulainen, Nucl. Phys. B **482**, 73 (1996) [hep-ph/9605235].
- [60] M. Dine and A. Kusenko, Rev. Mod. Phys. **76**, 1 (2003) [hep-ph/0303065].
- [61] T. Moroi, hep-ph/9503210.
- [62] O. Adriani *et al.* [PAMELA Collaboration], Phys. Rev. Lett. **105**, 121101 (2010) [arXiv:1007.0821 [astro-ph.HE]].
- [63] T. Delahaye and M. Grefe, JCAP **1312**, 045 (2013) [arXiv:1305.7183 [hep-ph]].

- [64] I. Cholis, JCAP **1109**, 007 (2011) [arXiv:1007.1160 [astro-ph.HE]].
- [65] M. Garny, A. Ibarra and D. Tran, JCAP **1208**, 025 (2012) [arXiv:1205.6783 [hep-ph]].
- [66] M. Cirelli and G. Giesen, JCAP **1304**, 015 (2013) [arXiv:1301.7079 [hep-ph]].
- [67] T. Sjostrand, S. Mrenna and P. Z. Skands, Comput. Phys. Commun. **178**, 852 (2008) [arXiv:0710.3820 [hep-ph]].
- [68] M. Grefe, arXiv:1111.6779 [hep-ph].
- [69] X. Huang, G. Vertongen and C. Weniger, JCAP **1201**, 042 (2012) [arXiv:1110.1529 [hep-ph]].
- [70] M. N. Mazziotta, F. Loparco, F. de Palma and N. Giglietto, arXiv:1203.6731 [astro-ph.IM].
- [71] M. Aguilar *et al.* [AMS Collaboration], Phys. Rev. Lett. **110**, no. 14, 141102 (2013).
- [72] O. Adriani *et al.* [PAMELA Collaboration], Phys. Rev. Lett. **111**, 081102 (2013) [arXiv:1308.0133 [astro-ph.HE]].
- [73] A. Ibarra and D. Tran, JCAP **0902**, 021 (2009) [arXiv:0811.1555 [hep-ph]].
- [74] A. Arbey, M. Battaglia, F. Mahmoudi and D. Martinez Santos, Phys. Rev. D **87**, 035026 (2013) [arXiv:1212.4887 [hep-ph]].
- [75] Y. Nir, arXiv:0708.1872 [hep-ph].
- [76] J. L. Feng and J. Kumar, Phys. Rev. Lett. **101**, 231301 (2008) [arXiv:0803.4196 [hep-ph]].
- [77] J. L. Feng and Y. Shadmi, Phys. Rev. D **83**, 095011 (2011) [arXiv:1102.0282 [hep-ph]].
- [78] T. Banks, J. D. Mason and D. O'Neil, Phys. Rev. D **72**, 043530 (2005) [hep-ph/0506015].

- [79] Y. Hochberg, E. Kuflik, H. Murayama, T. Volansky and J. G. Wacker, arXiv:1411.3727 [hep-ph].
- [80] Y. Hochberg, E. Kuflik, T. Volansky and J. G. Wacker, Phys. Rev. Lett. **113**, 171301 (2014) [arXiv:1402.5143 [hep-ph]].
- [81] A.I. Alekseev, Soviet Phys. JETP 7(1958) 826.
- [82] A.I. Alekseev, Soviet Phys. JETP 9 (1959) 1020.
- [83] P. Hoyer, arXiv:1402.5005 [hep-ph].
- [84] M. I. Eides, H. Grotch and V. A. Shelyuto, Phys. Rept. **342**, 63 (2001) [hep-ph/0002158].
- [85] E. Eichten, K. Gottfried, T. Kinoshita, J. Kogut, K. D. Lane, and T. -M. Yan, Phys. Rev. Lett. **36**, 1276 (1976)
- [86] T. Kawanai and S. Sasaki, Phys. Rev. D **85**, 091503 (2012) [arXiv:1110.0888 [hep-lat]].
- [87] L. Liu *et al.* [Hadron Spectrum Collaboration], JHEP **1207**, 126 (2012) [arXiv:1204.5425 [hep-ph]].
- [88] C. J. Morningstar and M. J. Peardon, Phys. Rev. D **60**, 034509 (1999) [hep-lat/9901004].
- [89] V. Mathieu, N. Kochelev and V. Vento, Int. J. Mod. Phys. E **18**, 1 (2009) [arXiv:0810.4453 [hep-ph]].
- [90] S. Prelovsek, arXiv:1310.4354 [hep-lat].
- [91] M. Jacob, G.C. Wick, Ann. Phys. **7**, 404 (1959)
- [92] F. Calogero, J.M. Charap, E.J. Squires, Ann. Phys. **25**, 325 (1963)
- [93] R. Jastrow, Phys. Rev. **81**, 636
- [94] J. Kang, M. A. Luty and S. Nasri, JHEP **0809**, 086 (2008) [hep-ph/0611322].
- [95] J. J. Sakurai, *Modern Quantum Mechanics*, Pearson, 1994

- [96] Gondolo, Gelmini, Nucl. Phys. B 360 (1991) 145
- [97] K. Garrett and G. Duda, Adv. Astron. **2011**, 968283 (2011) [arXiv:1006.2483 [hep-ph]].
- [98] Brau. Fabian, arXiv:math-ph/0401023.
- [99] E. Eichten, K. Gottfried, T. Kinoshita, J. Kogut, K. D. Lane, and T. -M. Yan, Phys. Rev. Lett. 34, 369
- [100] Shmuel Nussinov, Melissa A. Lampert (Tel Aviv U.). Nov 1999. 81 pp. Published in Phys.Rept. 362 (2002) 193-301 DOI: 10.1016/S0370-1573(01)00091-6